



HAL
open science

Boundary and VSL Control for Large-Scale Urban Traffic Networks

Liudmila Tumash, Carlos Canudas de Wit, Maria Laura Delle Monache

► **To cite this version:**

Liudmila Tumash, Carlos Canudas de Wit, Maria Laura Delle Monache. Boundary and VSL Control for Large-Scale Urban Traffic Networks. 2021. hal-03167733v1

HAL Id: hal-03167733

<https://hal.science/hal-03167733v1>

Preprint submitted on 12 Mar 2021 (v1), last revised 24 Oct 2021 (v2)

HAL is a multi-disciplinary open access archive for the deposit and dissemination of scientific research documents, whether they are published or not. The documents may come from teaching and research institutions in France or abroad, or from public or private research centers.

L'archive ouverte pluridisciplinaire **HAL**, est destinée au dépôt et à la diffusion de documents scientifiques de niveau recherche, publiés ou non, émanant des établissements d'enseignement et de recherche français ou étrangers, des laboratoires publics ou privés.

Boundary and VSL Control for Large-Scale Urban Traffic Networks

Liudmila Tumash, Carlos Canudas-de-Wit, *Fellow, IEEE* and Maria Laura Delle Monache, *Member, IEEE*

Abstract—This paper presents a unique method that considerably simplifies control design for traffic systems evolving in large-scale networks. In particular, we present a coordinate transformation that translates a 2D continuous traffic model based on a conservation law into a continuous set of equations with a structure similar to the classical LWR equation. Then for this system we explicitly design a boundary controller that drives the state to any space- and time-dependent desired trajectory. The desired state admits traffic regimes switching, i.e., it can be partially in free-flow and partially congested. Then we pose a different control task of stabilizing a system to quite any space-varying equilibrium. For that we design a variable speed limit (VSL) controller elaborating intrinsic properties of the model. The main peculiarity of both controls is that they require only the knowledge about the network geometry and the fundamental diagram. We validate the results numerically using the network of Grenoble.

Index Terms—boundary control, Hamilton-Jacobi, partial differential equations, urban traffic control, variable speed limit.

I. INTRODUCTION

CONTINUING urbanization caused by ever-growing population of the planet implies a growing demand for transportation. This entails formation of severe congestions that cost people hundreds of hours per year and that also have a significant negative impact on the environment. This requires the development of novel models and techniques able to predict traffic flow propagation and, thus, enhance the total travelling time for drivers by minimizing congestions.

The most common and simple model to describe traffic behaviour is the LWR model presented by Lighthill, Whitham [2] and Richards [3] in the fifties. This macroscopic model describes temporal evolution of aggregated quantities (traffic density and kinematic wave speed) as fluids. In particular, the LWR model is based on the conservation principle, where the

conserved quantity is the number of cars. Mathematically, this model is a first-order hyperbolic PDE with a concave flow function that represents an empirical relation between flow and density, see [25], [34] for a review on flow-density functions.

However, the LWR model was originally designed to describe traffic flow on a single infinite road. Thus, additional conditions and constraints had to be imposed in order to model traffic flow on networks that consist of links (roads) and nodes (junctions). A methodology for intersection modelling within LWR framework was proposed, e.g., in [18]. For the general theory of traffic flow on networks see [20]. The Cauchy problem for complex networks (with more than two in-coming and out-coming roads at junctions) was considered in [27].

The main challenge in this link-level (discrete) representation of traffic networks is a large computational time that significantly exaggerates validation of large networks consisting of thousands of links [14]. Alternatively, for two-dimensional modelling of traffic flow one can use continuous models. These models are used to describe traffic flow on networks having a large surface without spending too much computational effort. Another advantage of continuous models is that they require much less data than those needed under discrete modelling approach, e.g., road-by-road models.

The first works proposing continuous models to describe transportation networks in terms of aggregated variables appeared several decades ago, see [6], [8], [9]. These early models, however, failed in capturing the traffic flow dynamics in a rush hour due to the lack of any knowledge on a flow-density function. The existence of a Macroscopic Fundamental Diagram (MFD) in congested urban regions has been observed empirically [24], and further it was generalized in [23]. This discovery led to appearance of reservoir models (also called accumulation models), which describe the traffic state as evolution of the total number of cars depending on inflows and outflows at the zone's boundary. For a detailed review on Dynamic Traffic Assignment models using MFD see [39].

The main drawback of MFD-based models is that in case of heterogeneous links (having different levels of congestion), MFD might not be well-defined. To overcome this problem, [32], [35] presented partitioning algorithms to divide an urban area into multiple zones such that each of them has its own well-defined MFD. However, partitioning depends on the current level of congestion in each zone, which makes these accumulation models not adaptive to changes in traffic conditions, see also [40] for more details.

An alternative way to describe the propagation of urban

Manuscript received October 24, 2019; revised October 1, 2020. This work is a part of Scale-FreeBack project that received funding from the European Research Council (ERC) under the European Unions Horizon 2020 research and innovation programme (grant agreement N 694209).

L. Tumash is with Univ. Grenoble Alpes, CNRS, Inria, Grenoble INP, GIPSA-lab, 38000 Grenoble, France (email: liudmila.tumash@gipsa-lab.fr).

C. Canudas-de-Wit is with Univ. Grenoble Alpes, CNRS, Inria, Grenoble INP, GIPSA-lab, 38000 Grenoble, France (email: carlos.canudas-de-wit@gipsa-lab.grenoble-inp.fr).

M. L. Delle Monache is with Univ. Grenoble Alpes, Inria, CNRS, Grenoble INP, GIPSA-lab, 38000 Grenoble, France (email: ml.dellemonache@inria.fr).

traffic in a two-dimensional plane is to use models based on 2D conservation laws, whose state variable is traffic density, see [39] for a review. Recently, [37] proposed an extension of the original LWR model to two dimensions assuming that the traffic flow direction is determined by geometry and infrastructure of the underlying network only. This dependence is captured by introducing space-dependence into the flow-density function.

Usually when it comes to control design for a transportation network, the main goal is to improve the overall network efficiency. There exists a vast choice on literature devoted to the practical network control techniques, such as routing of traffic [17], traffic light control [33], ramp metering [10], variable speed limits [26], [36], see also [13] for a review. However, most of them are based on the first-discretize-then-optimize procedure or require using much of traffic data.

In this paper we propose a new technique that brings a continuous 2D conservation law model into a simple form. This modified system will be used for a pure analytic control design, for which we will use information only on inflows and outflows at domain's boundaries and on network infrastructure and geometry. We will then propose two different control designs to achieve different control goals.

Our main contributions are the following:

- 1) We present a method of transforming a 2D-LWR [37] into a continuous set of 1D systems, which enables an explicit elaboration of strategies for various control tasks to solve on large-scale networks.
- 2) We present the first explicitly derived boundary controller for a 2D conservation law model that is able to track a space- and time-dependent trajectory that allows shocks. For this we used the Hamilton-Jacobi framework, as it was done in [42], but extending it to 2D and handling *space-dependence* of the fundamental diagram. This means that instead of the classical Lax-Hopf formula, we had to apply the viability theory to the solution of a Hamilton-Jacobi-Moskowitz problem with a space-dependent Hamiltonian explained in [30], [29]. There also exists another boundary controller for 2D-LWR [41], where, however, the desired state was stationary and restricted to be in the same traffic regime as the initial traffic state.
- 3) The first explicitly derived VSL controller for a 2D conservation law that is applied continuously in space and time to drive a traffic state to almost any space-dependent desired equilibrium: we extend the work of [38] that was done for 1D-LWR for a spatially uniform equilibrium to two dimensions in order to achieve space-varying equilibriums. We also extend it by considering more general fundamental diagrams: space-dependent and non-monotonically depending on speed limits, which are more realistic (see [28]).

II. MODEL: 2D-LWR

Here we use a macroscopic model described in [37] that corresponds to the conservation law on a two-dimensional plane denoted by Ω with Γ being its boundary. This 2D-LWR model allows us to describe traffic on urban areas with a

preferred direction of motion (no loops). The state corresponds to the vehicle density $\rho(x, y, t) : \Omega \times \mathbb{R}^+ \rightarrow \mathbb{R}^+$, and we define the space-dependent transport flow function as

$$\vec{\Phi} = \Phi(x, y, \rho) \vec{d}_\theta(x, y), \quad (1)$$

where

$$\vec{d}_\theta = \begin{pmatrix} \cos(\theta(x, y)) \\ \sin(\theta(x, y)) \end{pmatrix} \quad (2)$$

is a vector defined by network's topology that determines the direction of transport flow. We will call it the *direction field*.

In (1) the flow magnitude $\Phi(x, y, \rho)$ is obtained from the *fundamental diagram* (FD), which is an empirical law relating flow and vehicle density. Mathematically, $\Phi(x, y, \rho) : \Omega \times \mathbb{R}^+ \rightarrow \mathbb{R}^+$ is a concave function with with the maximum $\phi_{max}(x, y) \forall (x, y) \in \Omega$ (*capacity*) achieved at the *critical density* $\rho_c(x, y)$, and the minimum is achieved at $\Phi(x, y, 0) = \Phi(x, y, \rho_{max}) = 0$ with $\rho_{max}(x, y)$ being the space-dependent traffic jam density. In the context of traffic modelling, we distinguish two different density regimes within the FD $\forall (x, y) \in \Omega$: the *free-flow regime* for $\rho(x, y) \in [0, \rho_c(x, y)]$ in which vehicles move freely with positive kinematic wave speed, and the *congested regime* for $\rho(x, y) \in (\rho_c(x, y), \rho_{max}(x, y)]$ characterized by a negative kinematic wave speed.

Now let us fix an initial condition $\rho_0(x, y)$ and boundary flows $\phi_{in}(x, y, t)$ and $\phi_{out}(x, y, t)$ and formulate the following initial boundary value problem (IBVP):

$$\begin{cases} \frac{\partial \rho(x, y, t)}{\partial t} + \nabla \cdot \vec{\Phi}(x, y, \rho(x, y, t)) = 0, \\ \vec{\Phi}(x, y, t) = \begin{cases} \phi_{in}(x, y, t) \vec{d}_\theta(x, y), & \forall (x, y) \in \Gamma_{in} \\ \phi_{out}(x, y, t) \vec{d}_\theta(x, y), & \forall (x, y) \in \Gamma_{out} \end{cases} \\ \rho(x, y, 0) = \rho_0(x, y), \end{cases} \quad (3)$$

where the upstream boundary $\Gamma_{in} \subset \Gamma$ is defined such that $\forall (x, y) \in \Gamma_{in}$: $\vec{n}(x, y) \cdot \vec{d}_\theta(x, y) > 0$, where $\vec{n}(x, y)$ is a unit normal vector to Γ_{in} oriented inside Ω . Similarly, for the downstream boundary $\Gamma_{out} \subset \Gamma$ we have $\forall (x, y) \in \Gamma_{out}$: $\vec{n}(x, y) \cdot \vec{d}_\theta(x, y) < 0$. The nabla operator in (3) is defined as:

$$\nabla = \left(\frac{\partial}{\partial x}, \frac{\partial}{\partial y} \right)$$

Further, inflows $\phi_{in}(x, y, t)$ and outflows $\phi_{out}(x, y, t)$ in (3) are defined as

$$\begin{cases} \phi_{in}(x, y, t) = \min \{u_{in}(x, y, t), S(\rho)\}, & (x, y) \in \Gamma_{in} \\ \phi_{out}(x, y, t) = \min \{D(\rho), u_{out}(x, y, t)\}, & (x, y) \in \Gamma_{out} \end{cases} \quad (4)$$

where $D(\rho)$ and $S(\rho)$ are demand and supply functions:

$$D(\rho) = \begin{cases} \phi(\rho), & \text{if } 0 \leq \rho \leq \rho_c, \\ \phi_{max}, & \text{if } \rho_c < \rho \leq \rho_{max}, \end{cases} \quad (5)$$

$$S(\rho) = \begin{cases} \phi_{max}, & \text{if } 0 \leq \rho \leq \rho_c, \\ \phi(\rho), & \text{if } \rho_c < \rho \leq \rho_{max}. \end{cases} \quad (6)$$

Finally, $u_{in}(t)$ and $u_{out}(t)$ are boundary controls corresponding to the demand function at the entry and the supply function at the exit of the road. Note that the conditions for inflows and outflows (4) are formulated as weak boundary conditions [21], which makes the whole IBVP given by (3) and (4) a well-posed problem.

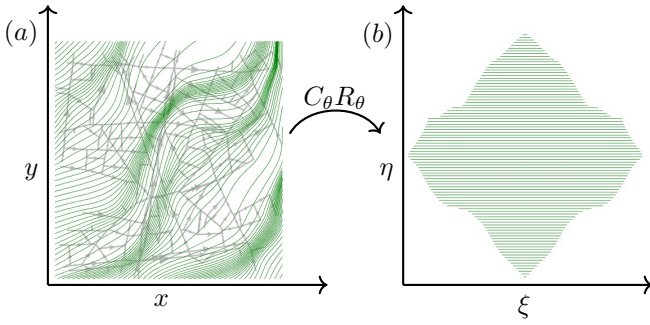


Fig. 1. Coordinate transformation mapping: (a) curved trajectories in Grenoble downtown in (x, y) -plane into (b) straight lines in (ξ, η) -plane.

Working with a continuous model such as (3) requires applying some interpolation techniques, since a real urban area is represented by a set of roads and junctions. Thus, we define $\forall(x, y) \in \Omega$ the direction field $\vec{d}_\theta(x, y)$ and the maximal velocity $v_{max}(x, y)$ by Inverse Distance Weighting, see [40], [37]. Thereby, we assume that $\vec{d}_\theta(x, y)$ depends on $v_{max}(x, y)$ and on the weighted distance between physical roads, where the weights can be tuned depending on the desired sensitivity of traffic flow to the mutual location of roads. Further, we also define the maximal density $\rho_{max}(x, y) \forall(x, y) \in \Omega$. We achieve that by placing every $6m$ a vehicle on every road of a network. Thereby, we assume that each such vehicle contributes to the global density with a Gaussian kernel with standard deviation $d_0 = 50m$ centred at its position (see [37]).

III. COORDINATE TRANSFORMATION

A. General idea

Due to (1), the direction of the flow field $\vec{\Phi}$ depends only on topology and not on the state. Thus, we are able to describe the trajectories along which the traffic flow evolves by defining the integral curves.

In the following we will perform a coordinate transformation that translates these integral curves into a set of straight parallel lines. Afterwards, each such line can be treated as a 1D system, which would significantly simplify any analysis of our 2D system (3). Thus, we introduce new coordinates (ξ, η) in a differential form:

$$\begin{pmatrix} d\xi \\ d\eta \end{pmatrix} = C_\theta(x, y) R_\theta(x, y) \begin{pmatrix} dx \\ dy \end{pmatrix}, \quad (7)$$

where $R_\theta(x, y)$ is a matrix that provides the rotation of the integral lines in (x, y) -plane and $C_\theta(x, y)$ is a scaling matrix providing that these lines have the same metric, see Fig. 1.

In order to produce Fig. 1a) we have used the real topology of Grenoble downtown (grey arrows) without loops such that flow crossings are impossible, i.e. there exists a preferred direction of motion. In particular, all roads need to be unidirectional. Thus, on global scale the motion on this network is oriented towards North-East of the city. The integral lines (in green) were built as tangents to the direction field \vec{d}_θ , which was constructed by following the procedure described in [37].

B. Intuition: straight lines

If originally we would deal with straight integral curves such that $\theta = 0 \forall(x, y) \in \Omega$ (as in Fig. 1b) and $C_\theta = R_\theta = \mathbb{I}$, then coordinates (ξ, η) would completely coincide with (x, y) . In this case, the vector field becomes $\vec{d}_\theta(\xi, \eta) = (1, 0)$, and by (1) we obtain:

$$\vec{\Phi} = \Phi(\xi, \eta, \rho) \begin{pmatrix} 1 \\ 0 \end{pmatrix}, \quad (8)$$

and with (8) the divergence in (3) yields:

$$\left(\frac{\partial}{\partial \xi}, \frac{\partial}{\partial \eta} \right) \begin{pmatrix} 1 \\ 0 \end{pmatrix} \Phi(\xi, \eta, \rho) = \frac{\partial \Phi(\xi, \eta, \rho)}{\partial \xi}. \quad (9)$$

Notice that in case of straight lines the divergence (9) contains only one term instead of two as it was in the original system (3). Thus, the flow evolves only along ξ coordinates, which are tangent to the flow motion. At the same time there is no motion in the orthogonal direction of η , which can be treated as a parameter (a label numbering the flow path). Afterwards, we can treat each such line of constant η as a 1D equation to solve different control tasks.

C. Coordinate transformation

After providing an intuitive explanation on how this coordinate transformation should work, we can define the matrices from (7). Then, we will perform the coordinate transformation of the original system (3) in order to turn it into a continuous set of 1D-LWR equations numbered by the flow path.

Thus, in (7) the rotation matrix is given by

$$R_\theta(x, y) = \begin{pmatrix} \cos(\theta(x, y)) & \sin(\theta(x, y)) \\ -\sin(\theta(x, y)) & \cos(\theta(x, y)) \end{pmatrix}, \quad (10)$$

and $C_\theta(x, y)$ is a diagonal scaling matrix given by

$$C_\theta(x, y) = \begin{pmatrix} \alpha(x, y) & 0 \\ 0 & \beta(x, y) \end{pmatrix} \quad (11)$$

where $\alpha(x, y)$ and $\beta(x, y)$ are positive and bounded scaling parameters needed for the existence of the coordinate transformation.

Lemma 1. Assume $\theta \in C^2 \forall(x, y) \in \Omega$ and $\alpha, \beta \in C^2$ such that they satisfy the following PDEs $\forall(x, y) \in \Omega$:

$$-\sin \theta \frac{\partial(\ln \alpha)}{\partial x} + \cos \theta \frac{\partial(\ln \alpha)}{\partial y} = \cos \theta \frac{\partial \theta}{\partial x} + \sin \theta \frac{\partial \theta}{\partial y} \quad (12)$$

and

$$\cos \theta \frac{\partial(\ln \beta)}{\partial x} + \sin \theta \frac{\partial(\ln \beta)}{\partial y} = \sin \theta \frac{\partial \theta}{\partial x} - \cos \theta \frac{\partial \theta}{\partial y}. \quad (13)$$

Then there exist functions $\xi(x, y)$ and $\eta(x, y)$ such that (7) is satisfied.

Proof. For any function in C^2 mixed partial derivatives must be equal by the Schwarz theorem. In our case this is equivalent to the invariance in the order of taking partial derivatives of ξ and η w.r.t. x and y , i.e.,

$$\frac{\partial}{\partial y} \left(\frac{\partial \xi(x, y)}{\partial x} \right) = \frac{\partial}{\partial x} \left(\frac{\partial \xi(x, y)}{\partial y} \right), \quad (14)$$

and

$$\frac{\partial}{\partial y} \left(\frac{\partial \eta(x, y)}{\partial x} \right) = \frac{\partial}{\partial x} \left(\frac{\partial \eta(x, y)}{\partial y} \right). \quad (15)$$

By applying (14) and (15) to (7) using the definitions (10) and (11) we obtain (12)-(13). Finally, ξ and η can be obtained by integrating (7). \square

Thus, $\alpha(x, y)$ and $\beta(x, y)$ being functions of $\vec{d}_\theta(x, y)$ only, can be computed from the network's topology.

D. Model in (ξ, η) -space

According to [1] we can apply the divergence formula to calculate $\nabla \cdot \vec{\Phi}$ in (ξ, η) -space:

$$\nabla \cdot \vec{\Phi} = \frac{1}{h_\xi h_\eta} \left[\frac{\partial (\vec{\Phi}_\xi h_\eta)}{\partial \xi} + \frac{\partial (\vec{\Phi}_\eta h_\xi)}{\partial \eta} \right], \quad (16)$$

where h_ξ and h_η are known as Lamé coefficients, which correspond to the lengths of the basis vectors in (ξ, η) -space:

$$\vec{h}_\xi = \left(\frac{\partial x}{\partial \xi}, \frac{\partial y}{\partial \xi} \right)^T \quad \text{and} \quad \vec{h}_\eta = \left(\frac{\partial x}{\partial \eta}, \frac{\partial y}{\partial \eta} \right)^T. \quad (17)$$

A detailed calculation of $\nabla \cdot \vec{\Phi}$ is given in [40], thus, we will directly state the result which reads:

$$\nabla \cdot \vec{\Phi} = \alpha \beta \left[\frac{\partial (\Phi/\beta)}{\partial \xi} \right]. \quad (18)$$

For simplicity we also introduce some new functions as:

$$\begin{aligned} \bar{\rho} &= \frac{\rho}{\alpha\beta}, \quad \bar{\Phi} = \frac{\Phi}{\beta}, \quad \bar{\phi}_{in} = \frac{\phi_{in}}{\beta}, \\ \bar{\phi}_{out} &= \frac{\phi_{out}}{\beta}, \quad \bar{S}_{out} = \frac{S_{out}}{\beta}, \quad \bar{D}_{in} = \frac{D_{in}}{\beta}, \end{aligned} \quad (19)$$

and, using (18) we can rewrite the original model (3) that now reads $\forall (\xi, \eta, t) \in \Omega \times \mathbb{R}^+$:

$$\begin{cases} \frac{\partial \bar{\rho}(\xi, \eta, t)}{\partial t} + \frac{\partial (\bar{\Phi}(\xi, \eta, \bar{\rho}))}{\partial \xi} = 0, \\ \bar{\phi}_{in}(\eta, t) = \min(\bar{u}_{in}(\eta, t), \bar{S}(\bar{\rho}(\xi_{min}(\eta), \eta, t))), \\ \bar{\phi}_{out}(\eta, t) = \min(\bar{D}(\bar{\rho}(\xi_{max}(\eta), \eta, t)), \bar{u}_{out}(\eta, t)), \\ \bar{\rho}(\xi, \eta, 0) = \bar{\rho}_0(\xi, \eta), \end{cases} \quad (20)$$

where

$$\xi_{min}(\eta) = \min_{\substack{(x,y) \in \Omega, \\ \eta(x,y) = \eta}} \xi(x, y), \quad \xi_{max}(\eta) = \max_{\substack{(x,y) \in \Omega, \\ \eta(x,y) = \eta}} \xi(x, y).$$

We can see that the traffic flow evolves only along lines of constant η in (ξ, η) -space. Thus, (20) is a continuous set of 1D-LWR equations each following a path parametrized by η .

Here we also introduce a notation for the minimal capacity along a line of constant η :

$$\min \bar{\phi}_{max}(\eta) = \min_{\xi \in [\xi_{min}(\eta), \xi_{max}(\eta)]} \bar{\phi}_{max}(\xi, \eta).$$

IV. BOUNDARY CONTROL

A. Problem Statement

Problem 1. Our objective is to design $\forall (\eta, t) \in \Omega \times \mathbb{R}^+$ boundary control laws $u_{in}(\eta, t)$ and $u_{out}(\eta, t)$ such that the vehicle density tracks a desired trajectory as $t \rightarrow \infty$.

In [42] a similar problem was posed for one road with no space dependence in the FD. Here we extend this result by doing it for a large urban area whose infrastructure is captured by space dependence in the FD, which makes its solution more technically involved.

B. Hamilton-Jacobi Formalism

It has been known [15], [16], [19] that an LWR type equation such as (20) can be solved exactly in the Hamilton-Jacobi formalism (H-J), which is an integral formulation of LWR. Its solution does not contain shocks, which enables us to analyze its properties more easily as it was done in [42].

In order to shift towards the H-J formalism, let us first introduce the cumulative number of vehicles $M(\xi, \eta, t)$ counted at a given position after a given time. This function is called the Moskowitz function named after Karl Moskowitz, an engineer who first used it to investigate traffic, although it was first mentioned only some decades later in [11]. Hence, in context of traffic, the H-J equation can also be called as Moskowitz PDE. Physically, the derivatives of $M(\xi, \eta, t)$ w.r.t. time and space correspond to flow and density, respectively:

$$\bar{\rho}(\xi, \eta, t) = -\frac{\partial M(\xi, \eta, t)}{\partial \xi}, \quad \bar{\phi}(\xi, \eta, t) = \frac{\partial M(\xi, \eta, t)}{\partial t}. \quad (21)$$

Further, we can use (21) to rewrite the fundamental flow-density relation $\bar{\Phi}(\xi, \eta, \rho(\xi, \eta, t)) = \phi(\xi, \eta, t)$ as

$$\frac{\partial M(\xi, \eta, t)}{\partial t} - \bar{\Phi} \left(\xi, \eta, -\frac{\partial M(\xi, \eta, t)}{\partial \xi} \right) = 0, \quad (22)$$

Equation (22) corresponds to the Hamilton-Jacobi equation. In terms of viability theory, $M(\xi, \eta, t)$ can also be called the *congestion function* (see [29]), since (22) can be considered as an optimal control problem minimizing a congestion functional $M(\xi, \eta, t)$, i.e., vehicles tend to minimize the traffic congestion by adapting their individual (microscopic) velocities to the kinematic wave velocity (a macroscopic quantity). In (22) $\bar{\Phi}$ plays the role of a Hamiltonian that governs the congestion function through the Moskowitz PDE.

Let us now establish how the congestion function is related to inflows and outflows of a studied area. We can simply do that by using the definitions from (21). Thereby, we set $M(\xi_{max}, \eta, t) = 0$, since congestion functions are decreasing functions of position and increasing functions of time, see chapter 14 of [29]. Finally, we obtain:

$$M(\xi, \eta, t) = \int_0^t \bar{\phi}_{out}(\eta, \tau) d\tau + \int_\xi^{\xi_{max}(\eta)} \bar{\rho}(\hat{\xi}, \eta, t) d\hat{\xi}, \quad (23)$$

or

$$M(\xi, \eta, t) = \int_{\xi_{min}(\eta)}^{\xi_{max}(\eta)} \bar{\rho}_0(\hat{\xi}, \eta) d\hat{\xi} + \int_0^t \bar{\phi}_{in}(\eta, \tau) d\tau - \int_{\xi_{min}(\eta)}^{\xi} \bar{\rho}(\hat{\xi}, \eta, t) d\hat{\xi}. \quad (24)$$

C. General Solution of H-J

Let us introduce the following IBVP problem for the Moskowitz PDE $\forall(\xi, \eta, t) \in \Omega \times \mathbb{R}^+$:

$$\begin{cases} \frac{\partial M(\xi, \eta, t)}{\partial t} - \bar{\Phi}\left(\xi, \eta, -\frac{\partial M(\xi, \eta, t)}{\partial \xi}\right) = 0, \\ M(\xi, \eta, 0) = M_{\text{Ini}}(\xi, \eta), \\ M(\xi_{\min}, \eta, t) = M_{\text{Up}}(\eta, t), \\ M(\xi_{\max}, \eta, t) = M_{\text{Down}}(\eta, t). \end{cases} \quad (25)$$

The relation of boundary conditions $M_{\text{Up}}(\eta, t)$ and $M_{\text{Down}}(\eta, t)$ to $\bar{\phi}_{\text{in}}(\eta, t)$ and $\bar{\phi}_{\text{out}}(\eta, t)$ is considered in detail in Appendix A.

The Moskowitz IBVP (22) can be solved analytically in accordance with the variational principle using only the initial condition function $M_{\text{Ini}}(\xi, \eta)$ and the boundary condition functions $M_{\text{Up}}(\eta, t)$ and $M_{\text{Down}}(\eta, t)$.

For convenience of notation, let us introduce the value condition function $\mathbf{c}(\xi, \eta, t) : \text{Dom}(\mathbf{c}) \rightarrow \mathbb{R}^+$, where $\text{Dom}(\mathbf{c}) = (\{\xi_{\min}(\eta), \xi_{\max}(\eta)\} \times \mathbb{R}^+) \cup ((\xi_{\min}(\eta), \xi_{\max}(\eta)) \times \{0\})$, which aggregates the initial and boundary conditions of (25):

$$\mathbf{c}(\xi, \eta, t) = \begin{cases} M_{\text{Ini}}(\xi, \eta) & t = 0, \\ M_{\text{Up}}(\eta, t) & \xi = \xi_{\min}(\eta), \\ M_{\text{Down}}(\eta, t) & \xi = \xi_{\max}(\eta). \end{cases} \quad (26)$$

Moreover, let us introduce a *Legendre-Fenchel transform of the flow* $\bar{\Phi}(\xi, \eta, \bar{\rho})$ as:

$$\begin{aligned} \forall v \in [-\bar{w}(\xi, \eta), \bar{v}_f(\xi, \eta)]: \\ L(\xi, \eta, v) = \sup_{\bar{\rho} \in [0, \bar{\rho}_{\max}(\xi, \eta)]} (\bar{\Phi}(\xi, \eta, \bar{\rho}) - v\bar{\rho}), \end{aligned} \quad (27)$$

where $\bar{v}_f(\xi, \eta)$ and $-\bar{w}(\xi, \eta)$ are related to the kinematic wave velocities for zero density and for the traffic jam density, respectively, i.e.:

$$\bar{v}_f(\xi, \eta) = \bar{\Phi}'(\xi, \eta, 0), \quad -\bar{w}(\xi, \eta) = \bar{\Phi}'(\xi, \eta, \bar{\rho}_{\max}).$$

Finally, the closed-form solution to (25) corresponding to the infimum among all viable evolutions that start at initial time $t - T$ and arrive at (ξ, η) at terminal time t reads as:

$$\begin{aligned} M(\xi, \eta, t) = \inf_{(T, v) \in S} \left\{ \mathbf{c}\left(\hat{\xi}(0), \eta, t - T\right) \right. \\ \left. + \int_0^T L\left(\hat{\xi}(\tau), \eta, v(\tau)\right) d\tau \right\}, \end{aligned} \quad (28)$$

where the infimum is taken over domain S defined as:

$$\begin{aligned} S = \left\{ (T, v) \mid T \in \mathbb{R}^+, v(\cdot) \in L^1(0, T), \dot{\hat{\xi}}(\tau) = v(\tau), \right. \\ \left. \hat{\xi}(T) = \xi, v(\tau) \in [-\bar{w}(\hat{\xi}(\tau), \eta), \bar{v}_f(\hat{\xi}(\tau), \eta)], \right. \\ \left. (\hat{\xi}(0), \eta, t - T) \in \text{Dom}(\mathbf{c}) \right\}. \end{aligned} \quad (29)$$

D. Explicit Solution for $t \rightarrow \infty$

For the calculation of the explicit solution to IBVP (25), we need first of all to specify the fundamental diagram, since it is necessary for the calculation of (27). There exist a lot of shapes for FDs in the literature, see for example Section 2 of

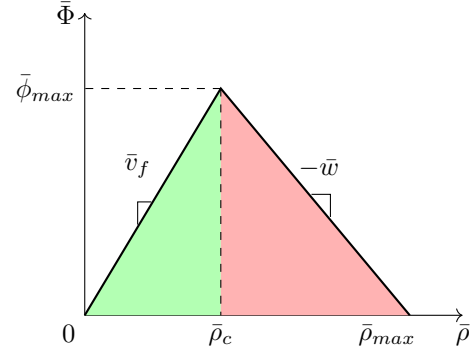


Fig. 2. Triangular FD for a fixed point of space: free-flow regime (area in green) and congested regime (area in red).

[34] for a brief review. Here we will use the triangular FD that is schematically illustrated in Fig. 2 for one space point only (its parameters might vary along both ξ and η coordinates). This shape of fundamental diagram was suggested in [12], and now it remains the most widespread one. It is defined as:

$$\bar{\Phi}(\xi, \eta, \bar{\rho}) = \begin{cases} \bar{v}_f \bar{\rho} & \bar{\rho} \in [0, \bar{\rho}_c], \\ -\bar{w}(\bar{\rho} - \bar{\rho}_{\max}) & \bar{\rho} \in (\bar{\rho}_c, \bar{\rho}_{\max}], \end{cases} \quad (30)$$

where $\bar{\rho}_c = \bar{\rho}_c(\xi, \eta)$, $\bar{\rho}_{\max} = \bar{\rho}_{\max}(\xi, \eta)$, $\bar{v}_f = \alpha v_f$ and $\bar{w} = \alpha w$. The critical density and the maximal flow are defined $\forall(\xi, \eta) \in \Omega$ as:

$$\bar{\rho}_c = \frac{\bar{w}}{\bar{v}_f + \bar{w}} \bar{\rho}_{\max}, \quad \bar{\Phi}_{\max} = \frac{\bar{v}_f \bar{w}}{\bar{v}_f + \bar{w}} \bar{\rho}_{\max}. \quad (31)$$

Further, throughout this paper we make the following assumptions:

Assumption 1. Inflows $\bar{\phi}_{\text{in}}(\eta, t)$ and outflows $\bar{\phi}_{\text{out}}(\eta, t)$ from the system (20) must satisfy $\forall(\eta, t) \in \Omega \times \mathbb{R}^+$:

$$\begin{aligned} \bar{\phi}_{\text{in}}(\eta, t) &\leq \min \bar{\Phi}_{\max}(\eta), \\ \bar{\phi}_{\text{out}}(\eta, t) &\leq \min \bar{\Phi}_{\max}(\eta). \end{aligned}$$

Moreover, there exists $\varepsilon > 0$ such that $\bar{\phi}_{\text{in}}(\eta, t)$ and $\bar{\phi}_{\text{out}}(\eta, t)$ additionally satisfy:

$$\begin{aligned} \int_t^{t+T_c(\eta)} \bar{\phi}_{\text{in}}(\eta, \tau) d\tau &\leq T_c(\eta) \min \bar{\Phi}_{\max}(\eta) - \varepsilon \quad \text{and} \\ \int_t^{t+T_c(\eta)} \bar{\phi}_{\text{out}}(\eta, \tau) d\tau &\leq T_c(\eta) \min \bar{\Phi}_{\max}(\eta) - \varepsilon, \end{aligned}$$

where $T_c(\eta)$ is the time needed for a solution evolving from one end of a line of constant η to reach the opposite end:

$$T_c(\eta) = \min \left\{ \int_{\xi_{\min}(\eta)}^{\xi_{\max}(\eta)} \frac{1}{\bar{v}_f(\hat{\xi})} d\hat{\xi}, \int_{\xi_{\min}(\eta)}^{\xi_{\max}(\eta)} \frac{1}{\bar{w}(\hat{\xi})} d\hat{\xi} \right\}. \quad (32)$$

It means that inflows and outflows at each line of constant η are not allowed to pass the minimal capacity of the corresponding line instantly and it must be strictly lower during the time interval given by $T_c(\eta)$. This assumption is necessary for the proof of Theorem 1.

Assumption 2. The solution of (20) is determined by the boundaries only, i.e., the initial conditions have left the system.

Remark 1. Note that if Assumption 1 is satisfied, then by taking $t \geq t_{min}$, where t_{min} was calculated in (90), Assumption 2 holds trivially, as it is shown in Appendix A.

Further, we use the variational principle (28) for the triangular FD (30) to calculate the solution to (25), which is quite technical and, therefore, we shift it to Appendix A. Thus, the solution $M(\xi, \eta, t)$ is obtained $\forall(\xi, \eta, t) \in \Omega \times [t_{min}, +\infty)$:

$$M(\xi, \eta, t) = \min \left\{ \int_0^{t-T_{v_f}(\xi, \eta)} \bar{\phi}_{in}(\eta, \tau) d\tau + \int_{\xi_{min}(\eta)}^{\xi_{max}(\eta)} \bar{\rho}_0(\hat{\xi}, \eta) d\hat{\xi}, \int_0^{t-T_w(\xi, \eta)} \bar{\phi}_{out}(\eta, \tau) d\tau + \int_{\xi}^{\xi_{max}(\eta)} \bar{\rho}_{max}(\hat{\xi}, \eta) d\hat{\xi} \right\}, \quad (33)$$

where

$$T_{v_f}(\xi, \eta) = \int_{\xi_{min}}^{\xi} \frac{1}{\bar{v}_f(\hat{\xi})} d\hat{\xi}, \quad T_w(\xi, \eta) = \int_{\xi}^{\xi_{max}} \frac{1}{\bar{w}(\hat{\xi})} d\hat{\xi}. \quad (34)$$

Note that $t \in [t_{min}, +\infty)$ implies that the effect of initial conditions should have left the system.

Remark 2. We widely use the solution (33) obtained in H-J formalism to analyse the properties of system (20) in order to design control. The major reason lies in weak boundary conditions given by (4), which imply that not any control can be imposed at the boundaries at any time. Thus, we use (33) to analyse the time during which controls might not be accepted by the system in terms of control restriction functions as it was done in [42].

E. Control Design

Theorem 1. Assume system (20) for which Assumptions 1 and 2 hold with the MF solution given by (33). Assume also the desired density $\bar{\rho}_d(\xi, \eta, t)$ and boundary flows $\bar{\phi}_{in_d}(\eta, t)$ and $\bar{\phi}_{out_d}(\eta, t)$ as in (20). Then if $\forall(\eta, t) \in \Omega \times \mathbb{R}^+$ the controls in (4) are set to

$$(1) \bar{u}_{in}(\eta, t) = \bar{\phi}_{in_d}(\eta, t) - ke(\eta, t), \quad t \in \mathbb{R}^+$$

$$(2) \bar{u}_{out}(\eta, t) = \bar{\phi}_{out_d}(\eta, t) + ke(\eta, t),$$

$$\text{where } e(\eta, t) = \int_{\xi_{min}}^{\xi_{max}} \left(\bar{\rho}(\hat{\xi}, \eta, t) - \bar{\rho}_d(\hat{\xi}, \eta, t) \right) d\hat{\xi} \quad \text{and } k > 0, \quad (35)$$

then $\forall a, b: \xi_{min}(\eta) \leq a < b \leq \xi_{max}(\eta)$ we obtain $\forall \eta \in \Omega$

$$\lim_{t \rightarrow \infty} \int_a^b \left(\rho(\hat{\xi}, \eta, t) - \rho_d(\hat{\xi}, \eta, t) \right) d\hat{\xi} = 0.$$

Proof. The proof is the same as for the 1D problem in [42] apart from a few differences listed in Appendix B. \square

Remark 3. Note that the integral convergence of densities stated in Theorem 1 implies that the state approximates the desired trajectory as time goes to infinity, since a and b can be arbitrarily close in space, i.e., $\rho \approx \rho_d$ as $t \rightarrow \infty$.

F. Numerical Example

Here we demonstrate the efficiency of our boundary control (35) applied to traffic in Grenoble downtown. We track a desired density profile that is space-dependent and periodic in time. The topology of the studied area in Grenoble is shown in grey in Fig. 4. However, we also need to assume that all the roads in Grenoble downtown are unidirectional, i.e., there exists some global direction towards North-East of the city. Maximal velocities on the majority of the roads are set to 30 km/h, while there are also few of them set to 50 km/h.

We discretize a two-dimensional plane as follows. First, we fix ξ and divide the interval $[\eta_{min}, \eta_{max}]$ into $n = 180$ curves. Then, we use a standard Godunov scheme for every $j \in \{1..n\}$ with a discretization step $\Delta\xi = 5m$. Note that curves j do not have equal lengths what implies that each j is divided into a different number of cells $m_j = \frac{\xi_{max_j} - \xi_{min_j}}{\Delta\xi}$. We use $i \in \{1..m_j\}$ to denote a discretization step for η . Finally, a time discretization step $\Delta t = 0.1$ provides that the CFL condition is satisfied. In order to compute the integral related to the feedback term in (35) we perform the Riemann summation for every j over all ξ cells, i.e., $i \in \{1..m_j\}$.

The use a triangular FD characterized by $\bar{\rho}_c(\xi, \eta) = \bar{\rho}_{max}(\xi, \eta)/3 \forall(\xi, \eta) \in \Omega$. Initially, the system that we want to control is given $\forall(\xi, \eta) \in \Omega$ by

$$\bar{\rho}_0(\xi, \eta) = \bar{\rho}_{max}(\xi, \eta).$$

We set the inflow demand $\bar{D}_{in_d}(\eta, t)$ and the output supply $\bar{S}_{out_d}(\eta, t)$ in the desired system to be periodic functions:

$$\bar{D}_{in_d}(\eta, t) = \min \bar{\phi}_{max}(\eta) \left[0.6 + 0.4 \sin \left(2\pi \left(\frac{t}{1200} + 2 \frac{\eta - \eta_{min}}{\eta_{max} - \eta_{min}} \right) \right) \right],$$

$$\bar{S}_{out_d}(\eta, t) = \min \bar{\phi}_{max}(\eta) \left[0.6 + 0.4 \sin \left(2\pi \left(\frac{t}{2400} + 2 \frac{\eta - \eta_{min}}{\eta_{max} - \eta_{min}} \right) \right) \right].$$

Hence, we have chosen these boundary flows to be smaller than the minimal capacity on each line of constant η . Note that these functions were chosen such to generate a desired trajectory ρ_d with the period $\tau = 2400$ seconds being in a mixed traffic regime, since we have a technique to handle mixed regimes which is mathematically the most tricky case.

We will demonstrate how does control given by (35) enhance the state if there is a feedback. The control is applied at the boundaries of the domain, and it physically corresponds to demand at the entry and supply of the exit, as illustrated in Fig. 3. Thus, we will compare two possible strategies:

- 1) Feedforward and feedback terms are used, i.e., $\forall \eta \in \Omega: \bar{u}_{in}(\eta, t) = \bar{\phi}_{in_d}(\eta, t) - ke(\eta, t)$ and $\bar{u}_{out}(\eta, t) = \bar{\phi}_{out_d}(\eta, t) + ke(\eta, t)$.
- 2) Only feedforward term is used (no feedback), i.e., $\forall \eta \in \Omega: \bar{u}_{in}(\eta, t) = \bar{\phi}_{in_d}(\eta, t)$ and $\bar{u}_{out}(\eta, t) = \bar{\phi}_{out_d}(\eta, t)$.

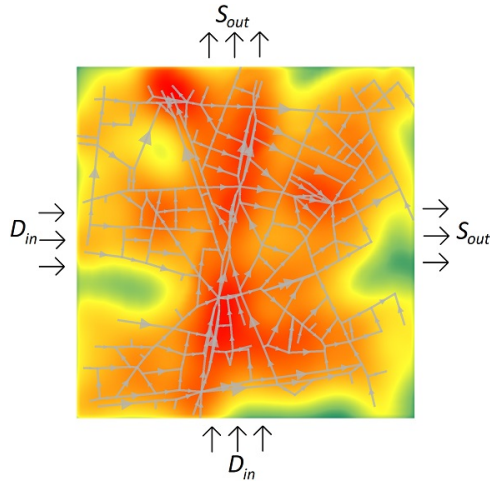


Fig. 3. The initial state to be controlled from the boundaries as indicated by black arrows.

In Fig. 4 the evolution of traffic density within the time interval of $2\tau = 4800$ seconds is shown. The middle column illustrates density controlled with the gain $k = 5 \cdot 10^{-5}$, i.e., strategy 1). The left column corresponds to the density evolution using only the boundary conditions of the desired system, i.e., strategy 2). The right column is related to the desired density with the initial and boundary conditions as described above. We can observe convergence of two profiles for the case with feedback that becomes visible already at $t = 2\tau$, while this does not happen for the case without feedback. Notice that the densities are drawn in (x, y) coordinates and without bars, thus, we had to rescale the functions and to perform the back transformation of coordinates.

In Fig. 5 the L_1 -norm of the error in the number of cars is depicted as a function of time for different control gains. It can be computed as follows:

$$\|\rho - \rho_d\|_1 = \int_{\eta_{min}}^{\eta_{max}} \int_{\xi_{min}(\eta)}^{\xi_{max}(\eta)} |\rho(\xi, \eta, t) - \rho_d(\xi, \eta, t)| d\xi d\eta. \quad (36)$$

We can clearly see that a higher control gain $k = 10^{-3}$ provides a higher convergence speed in comparison to $k = 5 \cdot 10^{-5}$. On the contrary, $k = 0$ will not achieve the goal even if we would start from an empty city without any cars until there is a difference in the initial conditions with the desired profile, which is usually always the case.

V. VARIABLE SPEED LIMIT CONTROL

Let us now demonstrate how to solve control tasks using variable speed limit (VSL) in a 2D-plane by stating a new problem in (ξ, η) -space.

A. Dependence of FD on Speed Limit

We introduce the following initial value problem (IVP):

$$\begin{cases} \frac{\partial \bar{\rho}(\xi, \eta, t)}{\partial t} + \frac{\partial \bar{\Phi}(\xi, \eta, \bar{\rho}(\xi, \eta, t), u(\xi, \eta, t))}{\partial \xi} = 0, \\ \bar{\rho}(\xi, \eta, 0) = \bar{\rho}_0(\xi, \eta), \end{cases} \quad (37)$$

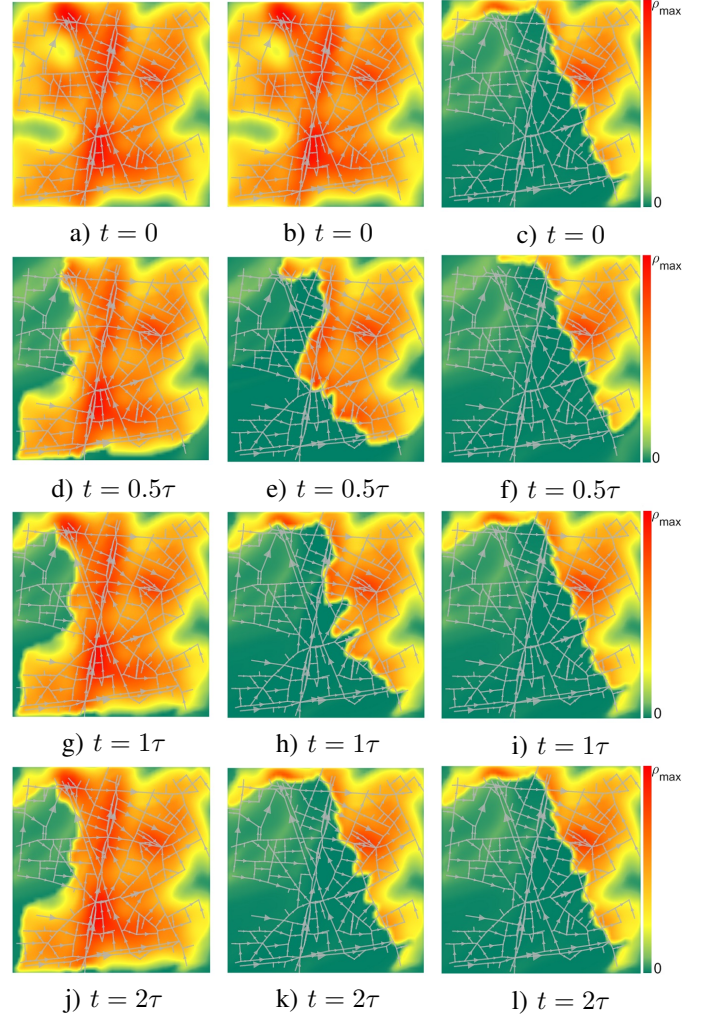


Fig. 4. Traffic control in Grenoble downtown. Right column: desired density $\rho_d(x, y, t)$; middle column: evolution of $\rho(x, y, t)$ with $k = 5 \cdot 10^{-5}$; left column: evolution of $\rho(x, y, t)$ with $k = 0$. All the plots represent snapshots made at: a) b) c) $t = 0$; d) e) f) $t = 0.5\tau$; g) h) i) $t = 1\tau$; j) k) l) $t = 2\tau$. The color bar denotes the ratio of the current density to the the maximal density all over the network.

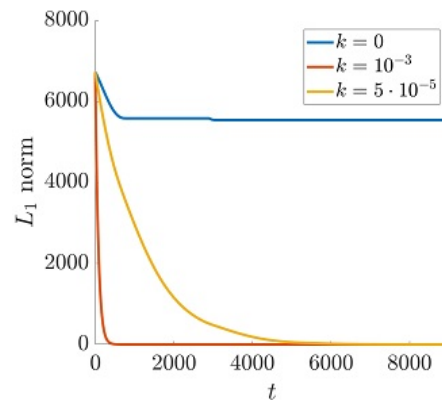


Fig. 5. L_1 error as a function of time for different control gains.

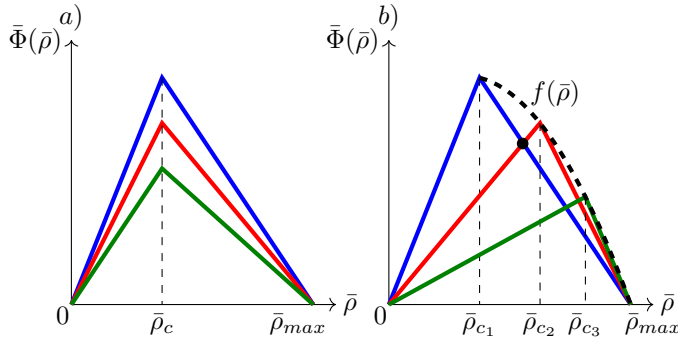


Fig. 6. Fundamental diagrams and their dependence on speed limits: a) monotonic dependence $\partial \bar{\Phi}(\xi, \eta, \bar{\rho}, u) / \partial u > 0$ used in [38]; b) dependence we assume here, i.e., possible increase of ρ_c for larger speed limits (from real data, see [28]). Blue line: $u = 1$. Red line: $u = 0.7$. Green line: $u = 0.5$. Bold dashed line: maximal flow function defined in (39).

where the flow function $\bar{\Phi}$ now depends also on $u(\xi, \eta, t) \in [0, 1]$, which is a control parameter representing the ratio of imposed speed limit to the maximal allowed speed: no speed limit is applied if $u = 1$, no movement is allowed if $u = 0$. Note that $\bar{\Phi}$ is concave with respect to $\bar{\rho}$, and $\bar{\Phi}$ is continuous in u . Moreover, $\bar{\Phi}(\xi, \eta, \bar{\rho}, 0) = \bar{\Phi}(\xi, \eta, 0, u) = 0$.

B. Contribution

Our contribution here was inspired by a previous work [38], however there are four major points that were not considered in [38], and thus will be addressed here:

- 1) *2D systems*: this is the first time that VSL control is applied on a large-scale network directly using the intrinsic properties of the model only, i.e. by analysing the structure of the 2D conservation law (no discretization).
- 2) *Space-dependent diagrams*: we extend the result of [38] by considering space-dependent diagrams, which imply space-dependent desired equilibrium profiles.
- 3) *Realistic FDs*: in [38] it was assumed that $\partial \bar{\Phi}(\xi, \eta, \bar{\rho}, u) / \partial u > 0$ holds, see Fig. 6a). This assumption was made for simplicity to avoid multivalued functions, i.e., there is only one value of u for each flow ϕ . In our work we omit this condition by allowing more general forms of FD. In general, applying speed limits can cause a shift of the critical density towards larger values in realistic fundamental diagrams as schematically depicted in Fig. 6b). There it is shown how VSL can increase flow for some densities in the congested regime (red and green FD). These VSL effects on the shape of FD were validated by real data collected from European VSL-equipped motorway, see [28]. In general, we have no restrictions on how FD must depend on VSL apart from $\bar{\Phi}(\xi, \eta, \bar{\rho}, 0) = 0$.
- 4) *Study the controller smoothness*: considering such a general class of fundamental diagrams may lead to irregular control policies. We investigate whether any conditions must be imposed on the functional dependence of FD on VSL in order to provide smoothness.

C. Problem Statement

We introduce the density error as:

$$\tilde{\rho}(\xi, \eta, t) := \bar{\rho}(\xi, \eta, t) - \bar{\rho}^*(\xi, \eta).$$

Let us also introduce the following notations:

$$\min_{\eta} \triangleq \min_{\eta \in [\eta_{min}, \eta_{max}]}, \quad \min_{\xi} \triangleq \min_{\xi \in [\xi_{min}(\eta), \xi_{max}(\eta)]}.$$

Problem 2. Given $\forall(\xi, \eta) \in \Omega$ the fundamental diagram $\bar{\Phi}(\xi, \eta, \bar{\rho}(\xi, \eta, t), u(\xi, \eta, t))$, initial density $\bar{\rho}_0(\xi, \eta)$ with dynamics governed by (37), find a VSL controller $u(\xi, \eta, t)$ such that $\forall(\xi, \eta) \in \Omega$:

$$\lim_{t \rightarrow \infty} \tilde{\rho}(\xi, \eta, t) = 0, \quad (38)$$

where $\bar{\rho}^*(\xi, \eta, t)$ is the deviation from an equilibrium $\bar{\rho}^*(\xi, \eta) \in (0, \bar{\rho}_{max}(\xi, \eta))$.

D. Control Design

Let us define a *maximal flow function* $f(\xi, \eta, \bar{\rho})$, which is the maximum possible flow that can be achieved at a given point for a given density over all the VSL values (see the thick dashed line in Fig. 8):

$$f(\xi, \eta, \bar{\rho}) = \max_{u \in [0, 1]} \bar{\Phi}(\xi, \eta, \bar{\rho}, u). \quad (39)$$

Moreover, we also introduce a multi-valued function $G(\xi, \eta, \bar{\rho}, \bar{\phi})$, which is the inverse function of the fundamental diagram with respect to the speed limit:

$$G(\xi, \eta, \bar{\rho}, \bar{\phi}) = \{u \in (0, 1] : \bar{\Phi}(\xi, \eta, \bar{\rho}, u) = \bar{\phi}\}. \quad (40)$$

In general, it is possible that several values of speed limits providing the same flow value, therefore $G(\xi, \eta, \bar{\rho}, \bar{\phi})$ for a fixed set of parameters represents a set, not a single value.

Theorem 2. Let the controller $u(\xi, \eta, t)$ be given by the following inclusion:

$$u(\xi, \eta, t) \in G(\xi, \eta, \bar{\rho}(\xi, \eta, t), \bar{\phi}(\xi, \eta, t)), \quad \text{with} \\ \bar{\phi}(\xi, \eta, t) = B(\xi, \eta, t) \min_{\xi} \frac{f(\xi, \eta, \bar{\rho}(\xi, \eta, t))}{B(\xi, \eta, t)} \quad (41)$$

$$\text{and } B(\xi, \eta, t) = 1 + \gamma \int_{\xi_{min}(\eta)}^{\xi} \bar{\rho}(\hat{\xi}, \eta, t) d\hat{\xi},$$

where

$$0 < \gamma < \min_{\eta} \left(\int_{\xi_{min}(\eta)}^{\xi_{max}(\eta)} \bar{\rho}_{max}(\hat{\xi}, \eta) d\hat{\xi} \right)^{-1}.$$

Then there exists $c > 0$ such that for every $\bar{\rho}_0(\xi, \eta) \in C^1(\Omega)$ the initial value problem (37) with $\bar{\rho}(\xi, \eta, 0) = \bar{\rho}_0(\xi, \eta)$ has a unique solution $\bar{\rho}(\xi, \eta, t) \in C^1(\Omega)$ which satisfies

$$\max_{(\xi, \eta) \in \Omega} |\tilde{\rho}(\xi, \eta, t)| \leq e^{-ct} \max_{(\xi, \eta) \in \Omega} |\tilde{\rho}(\xi, \eta, 0)| \quad \forall t > 0, \quad (42)$$

and, moreover, $\forall(\xi, \eta) \in \Omega$

$$\lim_{t \rightarrow \infty} \bar{\Phi}(\xi, \eta, \bar{\rho}(\xi, \eta, t), u(\xi, \eta, t)) = \min_{\xi} f(\xi, \eta, \bar{\rho}^*(\xi, \eta)). \quad (43)$$

Remark 4. The lower and upper bound on control gain γ are set such to guarantee that the flow $\bar{\phi}(\xi, \eta, t)$ is positive. This also yields that function $B(\xi, \eta, t)$ takes only positive values, i.e., $B(\xi, \eta, t) : \Omega \times \mathbb{R}^+ \rightarrow \mathbb{R}^+$.

Proof. First of all, we need to prove that the controller given by (41) is well-defined. Namely, we will show that the set $G(\xi, \eta, \bar{\rho}(\xi, \eta, t), \bar{\phi}(\xi, \eta, t))$ is not empty. Indeed, for all $(\xi, \eta) \in \Omega$ we get

$$\frac{\bar{\phi}(\xi, \eta, t)}{B(\xi, \eta, t)} = \min_{\xi} \frac{f(\xi, \eta, \bar{\rho}(\xi, \eta, t))}{B(\xi, \eta, t)} \leq \frac{f(\xi, \eta, \bar{\rho}(\xi, \eta, t))}{B(\xi, \eta, t)}, \quad (44)$$

and, thus, by positivity of $B(\xi, \eta, t)$, we get $\bar{\phi}(\xi, \eta, t) \in [0, f(\xi, \eta, \bar{\rho}(\xi, \eta, t))]$. This interval exactly corresponds to the range of function $\bar{\Phi}(\xi, \eta, \bar{\rho}(\xi, \eta, t), u(\xi, \eta, t))$ w.r.t. u , therefore the set function $G(\xi, \eta, \bar{\rho}(\xi, \eta, t), \bar{\phi}(\xi, \eta, t))$ is not empty.

Now we substitute

$$\bar{\Phi}(\xi, \eta, \bar{\rho}(\xi, \eta, t), u(\xi, \eta, t)) = B(\xi, \eta, t) \min_{\xi} \frac{f(\xi, \eta, \bar{\rho}(\xi, \eta, t))}{B(\xi, \eta, t)} \quad (45)$$

with $B(\xi, \eta, t)$ taken from (41) into the system (37) and obtain

$$\frac{\partial \bar{\rho}(\xi, \eta, t)}{\partial t} = -\gamma \bar{\rho}(\xi, \eta, t) \min_{\xi} \frac{f(\xi, \eta, \bar{\rho}(\xi, \eta, t))}{B(\xi, \eta, t)}. \quad (46)$$

This equation does not contain any partial space derivatives, and it has a stable equilibrium at zero. By [38] we obtain an exponential convergence with rate $c > 0$.

Finally, we see that if $\bar{\rho}(\xi, \eta, t) \rightarrow \bar{\rho}^*(\xi, \eta)$, then $B(\xi, \eta, t) \rightarrow 1$, and thus (45) results in

$$\bar{\Phi}(\xi, \eta, \bar{\rho}(\xi, \eta, t), u(\xi, \eta, t)) \rightarrow \min_{\xi} f(\xi, \eta, \bar{\rho}^*(\xi, \eta)),$$

which gives (43) and thus concludes the proof. \square

Remark 5. Condition (43) means that at time limit the highest possible constant flow is achieved for a given $\bar{\rho}^*$. Namely, by definition of (39), the following double inequality holds $\forall \eta \in \Omega$

$$\min_{\xi} \bar{\phi}(\xi, \eta, \bar{\rho}^*, 1) \leq \min_{\xi} f(\xi, \eta, \bar{\rho}^*) \leq \min_{\xi} \bar{\phi}_{max}(\xi, \eta), \quad (47)$$

where the left inequality implies that the same or higher traffic flow can be achieved with speed limits than those with $u = 1$.

E. Smoothness of VSL Controller

The controller (41) is defined via inclusion, and in general it can result in a highly discontinuous function in space. However, if we assume additional properties on how the flow function should depend on speed limit, we will obtain that $u(\xi, \eta, t)$ is differentiable almost everywhere.

Theorem 3. Assume that for any $(\xi, \eta) \in \Omega$ and $\bar{\rho} \in [0, \bar{\rho}_{max}(\xi, \eta)]$ the flow function $\bar{\Phi}(\xi, \eta, \bar{\rho}, u)$ is differentiable and either strictly concave in u (congested regime) or monotonic in u and reaches its maximum at $u = 1$ (free-flow regime). Further, assume Theorem 2 holds and $\bar{\rho}(\xi, \eta, t) \in C^1(\Omega)$. Then, $\forall t > 0$ the speed limit function $u(\xi, \eta, t)$ can have jump discontinuities only on a set of measure zero, and is differentiable everywhere else with respect to ξ .

Remark 6. This additional assumption on the functional dependence of $\bar{\Phi}(\xi, \eta, \bar{\rho}, u)$ on u can be interpreted as follows.

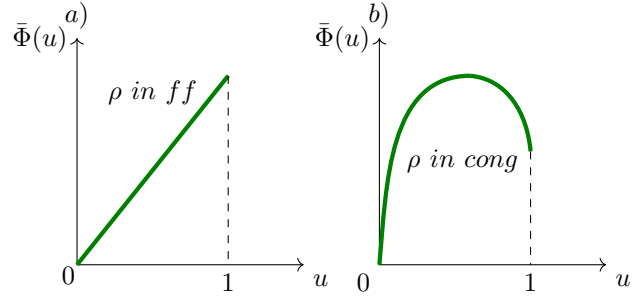


Fig. 7. FD as a function of u : a) monotonic dependence for a fixed ρ in free-flow; b) concave dependence for a fixed ρ in congested regime.

In the congested regime when the speed limit decreases, the flow can first increase for a fixed given density as in Fig. 7b), then it will decrease to zero as the speed limit approaches zero. For a free-flow density the flow is maximal for $u = 1$ and decreases monotonically as u decreases as in Fig. 7a).

Proof. For the proof of this theorem, we fix a time point t . Let us define a set $E \subset \Omega$ as

$$E = \{(\xi, \eta) \in \Omega : \bar{\phi}(\xi, \eta, t) = f(\xi, \eta, \bar{\rho}(\xi, \eta, t))\}. \quad (48)$$

This set consists of all points for which the obtained flow is the maximal one. Note that $\forall (\xi, \eta) \in E$ the speed limit value is unique due to the concavity of the fundamental diagram with respect to the speed limit function in the congested regime and due to the monotonicity in the free flow regime. Further, we can split this set as $E = E_0 \cup E_1 \cup E_+$ where E_1 consists of all open intervals of non-zero measure such that $u(\xi, \eta, t) = 1$, then E_+ consists of open intervals of non-zero measure with $u(\xi, \eta, t) < 1$ and E_0 has a measure zero.

Obviously, set E_1 is free of jumps because $u \equiv 1$ on it. Further, since the maximal flow on the set E_+ is achieved for $u < 1$, the density should be in congested regime, thus the fundamental diagram is strictly concave with respect to u in this set. Thus, the following must hold for every point in E_+ :

$$\frac{\partial \bar{\Phi}(\xi, \eta, \bar{\rho}(\xi, \eta, t), u(\xi, \eta, t))}{\partial u} = 0, \quad (49)$$

since the maximal flow is achieved with $u(\xi, \eta, t)$. Taking the partial derivative of (49) w.r.t. ξ for each η (recall that $\bar{\Phi}(\xi, \eta, \bar{\rho}, u)$ and $\bar{\rho}(\xi, \eta, t)$ are differentiable), we arrive at

$$\frac{\partial^2 \bar{\Phi}}{\partial u^2} \frac{\partial u}{\partial \xi} = -\frac{\partial^2 \bar{\Phi}}{\partial u \partial \xi} - \frac{\partial^2 \bar{\Phi}}{\partial u \partial \bar{\rho}} \frac{\partial \bar{\rho}}{\partial \xi},$$

with $\frac{\partial^2 \bar{\Phi}}{\partial u^2} < 0$. This can be viewed as a differential equation for u with respect to ξ , and thus $u(\xi, \eta, t)$ is differentiable on E_+ for each η .

Now let us investigate the set $\Omega \setminus E$. On this set $\bar{\phi}(\xi, \eta, t) < f(\xi, \eta, \bar{\rho}(\xi, \eta, t))$, therefore the flow is not maximal and the derivative of the fundamental diagram with respect to u is not zero. Then, taking the derivative of (45) w.r.t. ξ , we obtain

$$\frac{\partial \bar{\Phi}}{\partial \xi} + \frac{\partial \bar{\Phi}}{\partial \bar{\rho}} \frac{\partial \bar{\rho}}{\partial \xi} + \frac{\partial \bar{\Phi}}{\partial u} \frac{\partial u}{\partial \xi} = \frac{\partial B}{\partial \xi} \min_{\xi} \frac{f(\xi, \eta, \bar{\rho}(\xi, \eta, t))}{B(\xi, \eta, t)}, \quad (50)$$

where $\frac{\partial \bar{\Phi}}{\partial u}$ is not zero. This proves that $u(\xi, \eta, t)$ is differentiable on $\Omega \setminus E$.

Finally, combining these results, we obtain that $u(\xi, \eta, t)$ is differentiable on $\Omega \setminus E_0$, and E_0 is a set of measure zero. \square

Proposition 1. *In case of concave dependence on speed limits, $u(\xi, \eta, t)$ can sometimes be chosen from two values $G(\xi, \eta, \bar{\rho}(\xi, \eta, t), \bar{\phi}(\xi, \eta, t))$ for ρ being in congested regime, see Fig. 7 b). Then the most appropriate choice from the practical point of view is the minimal value, since it provides free-flow regime:*

$$u(\xi, \eta, t) := \min G(\xi, \eta, \bar{\rho}(\xi, \eta, t), \bar{\phi}(\xi, \eta, t)).$$

As an example, consider the intersection point (black dot) in Fig. 6b) corresponding to the flow-density pair that can be achieved using $u = 1$ and $u = 0.7$. In this case we should choose $u = 0.7$, since this provides free-flow regime and thus, a more smooth traffic motion.

F. Numerical Example

In order to construct a numerical example demonstrating how a VSL controller works on an urban network corresponding to Grenoble downtown, we should parametrize the shape of the fundamental diagram.

1) *Parametrization of Fundamental Diagram:* Let us assume that the basic shape of FD is triangular as in (30), which, however, should be modified due to the dependence on speed limits. We denote $\bar{v}_f(\xi, \eta)$ and $\bar{w}_1(\xi, \eta)$ as kinematic wave speeds for $u = 1$ in the free-flow and in the congested regime, respectively. We can assume a linear dependence of wave speeds on speed limits, e.g.,

$$\begin{cases} \bar{v}_f(\xi, \eta, u) = u \bar{v}_f(\xi, \eta), \\ \bar{w}(\xi, \eta, u) = \bar{w}_1(\xi, \eta) + (1 - u)\Delta\bar{w}(\xi, \eta), \end{cases} \quad (51)$$

where $\Delta\bar{w}(\xi, \eta)$ is the value expressing the effect of speed limit on the kinematic wave speed. Thus, if the speed limits are high ($u \ll 1$), drivers are moving slowly, and thus start braking late. Let us estimate the range of reasonable values for $\Delta\bar{w}(\xi, \eta)$ such that $\forall(\xi, \eta) \in \Omega$

$$\frac{\partial \bar{\phi}_{max}(\xi, \eta, u)}{\partial u} \geq 0. \quad (52)$$

Condition (52) means that it is not possible to enhance the maximal possible flow by applying speed limits, see (47). In the following we skip the dependence on (ξ, η) in notations. We insert $\bar{w}(u)$ and $\bar{v}_f(u)$ from (51) into (31) and get

$$\bar{\phi}_{max}(u) = \bar{v}_f \bar{\rho}_{max} \frac{u(\bar{w}_1 + (1 - u)\Delta\bar{w})}{\bar{w}_1 + \bar{v}_f u + (1 - u)\Delta\bar{w}}. \quad (53)$$

We take the partial derivative of (53) w.r.t. u and obtain

$$\frac{\partial \bar{\phi}_{max}(u)}{\partial u} = \frac{(\bar{w}_1 + (1 - u)\Delta\bar{w})^2 - u^2 \Delta\bar{w} \bar{v}_f}{(\bar{w}_1 + \bar{v}_f u + (1 - u)\Delta\bar{w})^2}. \quad (54)$$

We distinguish two different cases for which the nominator of (54) takes non-negative values $\forall u \in [0, 1]$:

- 1) Case $\Delta\bar{w} \leq 0$. Obviously, $\partial \bar{\phi}_{max}(u)/\partial u > 0$,
- 2) Case $\Delta\bar{w} > 0$. Then $\bar{w}_1 + (1 - u)\Delta\bar{w} \geq u\sqrt{\Delta\bar{w}\bar{v}_f} \Rightarrow \bar{w}_1 + \Delta\bar{w} \geq u(\Delta\bar{w} + \sqrt{\Delta\bar{w}\bar{v}_f})$.

In the worst case this inequality must be satisfied for $u = 1$, which results in

$$\Delta\bar{w} \leq \frac{\bar{w}_1^2}{\bar{v}_f}.$$

This expression yields the upper bound for $\Delta\bar{w}$. By the definition (51) and the fact that $\bar{w}(u)$ should be non-negative the lowest bound is $-\bar{w}_1$, thus, the range reads

$$\Delta\bar{w} \in \left[-\bar{w}_1, \frac{\bar{w}_1^2}{\bar{v}_f} \right].$$

For the numerical example we pick $\Delta\bar{w} = \bar{w}_1^2/\bar{v}_f$, since this value provides $\partial \bar{\phi}_{max}(u)/\partial u = 0$ at $u = 1$. From the physical viewpoint, this implies the largest possible influence of VSL on FD in the congested regime (the largest possible surface enclosed by the blue line in the congested regime and the thick dashed line in Fig. 8).

2) *Optimal Equilibrium:* The controller given by (41) is valid for any type of equilibrium $\bar{\rho}^*(\xi, \eta) \in (0, \bar{\rho}_{max}(\xi, \eta)) \forall(\xi, \eta) \in \Omega$. However, for the numerical example we want an optimal equilibrium $\bar{\rho}_{opt}^*$ that corresponds to the throughput maximization and, at the same time, to the density maximization, i.e., the highest possible number of cars will pass the system at the maximal flow. Thereby, the number of cars can be increased due to the change in the shape of fundamental diagram caused by $u(\xi, \eta, t)$ as it is shown in Fig. 8.

The method to compute exactly the equilibrium profiles providing the maximal flow in the system was presented in [41]. However, it was done for $u = 1$, i.e., no speed limits were applied. With the help of speed limits we are now able to extend the result of [41] by maximizing the number of vehicles that can pass the system at the maximal flow.

In particular, we want to find $\forall(\xi, \eta) \in \Omega$ speed limits $u_{opt}(\xi, \eta)$ such that

$$\bar{\phi}_{max}(\xi, \eta, u_{opt}) = \min_{\xi} \bar{\phi}_{max}(\xi, \eta, 1),$$

which implies that

$$\bar{\rho}_{opt}^*(\xi, \eta) = \bar{\rho}_c(\xi, \eta, u_{opt}).$$

Thus, the desired equilibrium corresponds to the critical density achieved for u_{opt} . In terms of Fig. 8 this means that if $\min_{\xi} \bar{\phi}_{max}(u = 1) = \bar{\phi}_{max}^*$ for some $(\xi, \eta) \in \Omega$, then u_{opt} is such that $\bar{\rho}_{opt}^* = \bar{\rho}_c^*$. Thus, the maximal possible flow remains the same $\bar{\phi}_{max}^*$, while the density is increased, since $\bar{\rho}_c^* > \bar{\rho}_1$. It is also worth noting that at the desired equilibrium vehicles operate only at the critical density, i.e., there will be no congestions in the whole area.

In the following we skip (ξ, η) in the notations for simplicity. In order to find $u_{opt} \forall(\xi, \eta) \in \Omega$, we use (53) and (31), and obtain

$$\bar{\phi}_{max}(u_{opt}) = \bar{v}_f \frac{\bar{v}_f + \bar{w}_1}{\bar{w}_1} \bar{\rho}_c \frac{u_{opt}(\bar{w}_1 + (1 - u_{opt})\Delta\bar{w})}{\bar{w}_1 + \bar{v}_f u_{opt} + (1 - u_{opt})\Delta\bar{w}}, \quad (55)$$

where $\bar{\rho}_c$ corresponds to the critical density as in (31) for $\bar{v}_f = \bar{v}_f$ and $\bar{w} = \bar{w}_1$.

Further, we use $\bar{\rho}_c \bar{v}_f = \bar{\phi}_{max_1}$ with $\bar{\phi}_{max_1}$ being the highest possible flow for some $(\xi, \eta) \in \Omega$ reached with $u = 1$,

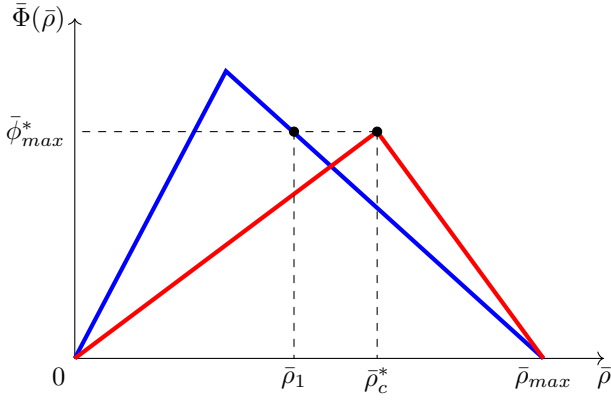


Fig. 8. Blue line: FD for $u = 1$. Red line: FD for $u = u_{opt}$.

and $\Delta\bar{w} = \bar{w}_1^2/\bar{v}_{f_1}$ to rewrite (55) as

$$\begin{aligned}\bar{\phi}_{max}(u_{opt}) &= \bar{\phi}_{max_1}(\bar{v}_{f_1} + \bar{w}_1) \frac{u_{opt} \left(1 + (1 - u_{opt}) \frac{\bar{w}_1}{\bar{v}_{f_1}}\right)}{\bar{w}_1 + \bar{v}_{f_1} u_{opt} + \frac{\bar{w}_1}{\bar{v}_{f_1}} - u_{opt} \frac{\bar{w}_1}{\bar{v}_{f_1}}} \\ &= \bar{\phi}_{max_1} \frac{u_{opt} (\bar{v}_{f_1} + (1 - u_{opt})\bar{w}_1)}{\bar{w}_1 + (\bar{v}_{f_1} - \bar{w}_1) u_{opt}}.\end{aligned}\quad (56)$$

Let us now introduce $\lambda(\xi, \eta) \in (0, 1]$ to denote $\forall(\xi, \eta) \in \Omega$ the ratio of the flow that needs to be achieved at the optimal equilibrium to the maximal possible flow achieved at $u = 1$:

$$\lambda(\xi, \eta) = \frac{\min_{\xi} \bar{\phi}_{max}(\xi, \eta, 1)}{\bar{\phi}_{max}(\xi, \eta, 1)}.$$

From (56) we get the following equation $\forall(\xi, \eta) \in \Omega$ to be solved for u_{opt} :

$$\lambda = \frac{u_{opt} (\bar{v}_{f_1} + (1 - u_{opt})\bar{w}_1)}{\bar{w}_1 + (\bar{v}_{f_1} - \bar{w}_1) u_{opt}}.$$

This is a quadratic equation with respect to u_{opt} , which yields two solutions. We pick up the one with minus, since this guarantees that u_{opt} remains below 1:

$$u_{opt} = \frac{\mu + 1 - \lambda(\mu - 1) - \sqrt{(\mu + 1 - \lambda(\mu - 1))^2 - 4\lambda}}{2}, \quad (57)$$

with $\mu = \bar{v}_{f_1}/\bar{w}_1$. Finally, the optimal equilibrium is the critical density defined in (31) obtained for u_{opt} from (57):

$$\bar{\rho}_{opt}^* = \frac{\bar{w}(u_{opt})}{\bar{v}_f(u_{opt}) + \bar{w}(u_{opt})} \bar{\rho}_{max}, \quad (58)$$

where $\bar{v}_f(u_{opt})$ and $\bar{w}(u_{opt})$ should be taken from (51) for $u = u_{opt}$ and $\Delta\bar{w} = \bar{w}_1^2/\bar{v}_{f_1}$.

3) Numerical Setup: As a network we again take the downtown of Grenoble. All the infrastructure parameters and the two-dimensional discretization scheme are exactly the same as described in the previous numerical example.

We use a triangular FD with $\bar{\rho}_c(\xi, \eta) = \bar{\rho}_{max}(\xi, \eta)/3$ $\forall(\xi, \eta) \in \Omega$. At $t = 0$ the system is given $\forall(\xi, \eta) \in \Omega$ by

$$\bar{\rho}_0(\xi, \eta) = 3\bar{\rho}_{max}(\xi, \eta)/4,$$

thus, it is quite congested. The inflow demand $\bar{D}_{in}(\eta, t)$ and the output supply $\bar{S}_{out}(\eta, t)$ are set to the maximal possible flows for each line of constant η for all times:

$$\bar{D}_{in}(\eta, t) = \min \bar{\phi}_{max}(\eta), \quad \bar{S}_{out}(\eta, t) = \min \bar{\phi}_{max}(\eta),$$

which are the only possible values if we want to maximize the throughput.

The desired optimal equilibrium is found as described above (58), and it is depicted in Fig. 9b). This state is characterized by the maximal possible flow through the system achieved for the maximal possible number of vehicles.

Let $j \in [1, \dots, n]$ and $i \in [1, \dots, m_j]$ be the cell indices as described in the previous example and $k \in \mathbb{Z}^+$ is the time index. In order to apply VSL control we first compute on each time step $u_{i,j}(k)$ as in the algorithm (41), and then we update the density using the Godunov scheme. Let us fix j (the cell number of η), then the numerical scheme reads:

$$\begin{aligned}\bar{\rho}_i(k+1) &= \bar{\rho}_i(k) + \frac{\Delta t}{\Delta \xi} \left(\min \{ \bar{D}_{i-1}(k), \bar{S}_i(k) \} \right. \\ &\quad \left. - \min \{ \bar{D}_i(k), \bar{S}_{i+1}(k) \} \right),\end{aligned}$$

where $\bar{D}_i(k)$ and $\bar{S}_i(k)$ are demand and supply functions, respectively, that depend on VSL for each k

$$\begin{aligned}\bar{D}_i &= \begin{cases} \bar{\phi}_i, & \text{if } 0 \leq \bar{\rho}_i \leq \bar{\rho}_{c_i}, \\ \bar{\phi}_{max_i}, & \text{if } \bar{\rho}_{c_i} < \bar{\rho}_i \leq \bar{\rho}_{max_i}, \end{cases} \\ \bar{S}_i &= \begin{cases} \bar{\phi}_{max_i}, & \text{if } 0 \leq \bar{\rho}_i \leq \bar{\rho}_{c_i}, \\ \bar{\phi}_i, & \text{if } \bar{\rho}_{c_i} < \bar{\rho}_i \leq \bar{\rho}_{max_i}, \end{cases}\end{aligned}$$

where $\bar{\phi}_i = \bar{\Phi}_i(\xi_i, \eta_j, u_{i,j})$, $\bar{\phi}_{max_i} = \bar{\phi}_{max}(\xi_i, \eta_j, u_{i,j})$ and $\bar{\rho}_{c_i} = \bar{\rho}_c(\xi_i, \eta_j, u_{i,j})$ are all functions of VSL $u_{i,j}$ as in (51).

Note that in (41) there exists an upper bound for γ that guarantees that $B(\xi, \eta, t) > 0$ $\forall(\xi, \eta, t) \in \Omega \times \mathbb{R}^+$. However, one can accelerate convergence by choosing the maximal possible $\gamma(\eta, t)$ for each line of constant η and for each time.

Thus, we will use two different control gains:

- 1) A constant control gain $\gamma = 0.14$ that matches the bounds stated in Theorem 2 in this setup.
- 2) A time- and space-varying control gain $\gamma(\eta, t)$:

$$\gamma(\eta, t) = \frac{1 - \epsilon}{\max \left\{ -\min_{\eta} \int_{\xi_{min}(\eta)}^{\xi_{max}(\eta)} \tilde{\rho}(\hat{\xi}, \eta, t) d\hat{\xi}, \delta \right\}}, \quad (59)$$

where $\delta > 0$ is chosen to get $\gamma > 0$ even if the minimum is positive (since the arbitrarily large γ can be used), and $\epsilon > 0$ provides the lower bound for $B(\xi, \eta, t)$.

Fig. 9c) - f) illustrates the temporal evolution of traffic density under the VSL control with a time-varying gain given by (59) with $\epsilon = 0.01$ and $\delta = 0.1$. Thereby, at every time demand and supply functions at domain boundaries are set to the maximal possible throughput corresponding to the desired flow in the system. We observe that the state converges to the desired equilibrium, which becomes visible already after $t = 2$ hours of real time.

Remark 7. Notice that at the desired equilibrium the critical density at each point of space will be higher than at initial

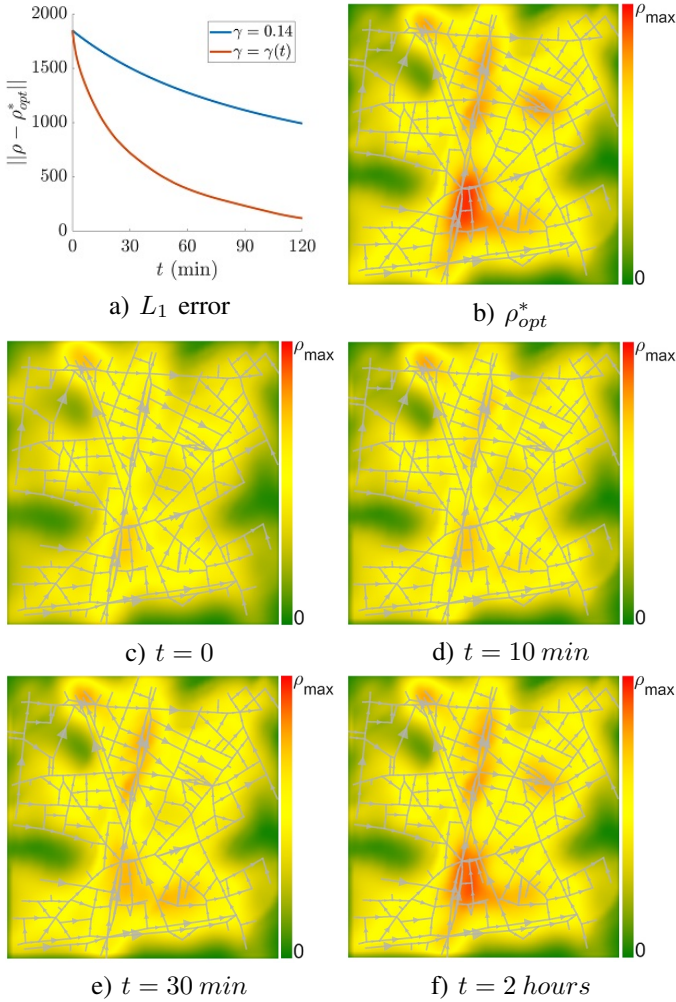


Fig. 9. a) L_1 error as a function of time for different control gains; b) the desired optimal equilibrium as in (58). Traffic flow control by VSL in Grenoble downtown. Density $\rho(x, y, t)$ at: c) $t = 0$; d) $t = 10$ min; e) $t = 30$ min; f) $t = 2$ hours. The color bar denotes the ratio of the current density to the maximal density all over the network.

time due to VSL control as in (58). Moreover, the steady-state critical density is determined by the network topology.

Further, we compute L_1 -norm of the error in the number of cars as in (36) with $\rho_{opt}^*(\xi, \eta)$ as a desired state. Its temporal evolutions for two different control gains are shown in Fig. 9a). As in the previous example, we again observe that a larger control gain (59) provides a higher convergence speed in comparison to the constant $\gamma = 0.14$. Recall that as soon as we start applying control, the traffic system is completely set to the free-flow regime, since we always choose the minimal VSL value (see Proposition 1).

VI. CONCLUSIONS

We have introduced and explained the coordinate transformation that allows us to treat a 2D traffic system as a 1D system to solve different control tasks. Mathematically, it means that instead of two partial derivatives with respect to space the modified system has only one. We were able to do that since the 2D LWR model considered in this paper has a

special property, i.e., traffic flow evolves along the lines that depend only on the network topology and not on the state.

Further, we have presented two control design techniques to solve different problems. The first controller is applied at domain's boundaries, and it is used to track a space- and time-dependent trajectory that can be in any traffic regime. We used the viability solution of the Hamilton-Jacobi PDE to prove that the goal will be achieved even if controls can not be directly imposed at the boundaries. The second controller was a VSL controller that was applied continuously in space in the whole domain. We used it to stabilize the system to a desired space-dependent equilibrium. We have also investigated how to design an optimal desired equilibrium that corresponds to the throughput maximization achieved for the maximal possible number of cars. The numerical examples for both controllers were performed using the topology of Grenoble, and stay in good agreement with the theory.

For the future studies it would be useful to perform this analysis for a model that allows multiple directions in the network, since assuming a network without loops was the main limitation of this work.

APPENDIX I SOLUTION OF MOSKOWITZ PDE

In the following we will skip writing η in the arguments to make the notations less heavy. Let us here assume that we solve the Moskowitz PDE explicitly for each line of constant η . Also for simplicity we will omit bars in the notations.

The Legendre transform (27) of a triangular FD is

$$L(\xi, v) = \phi_{max}(\xi) - \rho_c(\xi)v \quad \forall v \in [-w(\xi), v_f(\xi)]. \quad (60)$$

Now we can determine the value condition function which implies the calculation of $M_{Up}(t)$, $M_{Down}(t)$ and $M_{Ini}(\xi)$:

$$M_{Up}(t) = c(\xi_{min}, t) = \int_0^t \phi_{in}(\tau) d\tau + \int_{\xi_{min}}^{\xi_{max}} \rho_0(\hat{\xi}) d\hat{\xi}. \quad (61)$$

$$M_{Down}(t) = c(\xi_{max}, t) = \int_0^t \phi_{out}(\tau) d\tau. \quad (62)$$

$$M_{Ini}(\xi) = c(\xi, 0) = \int_{\xi}^{\xi_{max}} \rho_0(\hat{\xi}) d\hat{\xi}. \quad (63)$$

Thus, we need to calculate the solutions $M_{Up}(\xi, t)$, $M_{Down}(\xi, t)$ and $M_{Ini}(\xi, t)$ associated to given conditions $M_{Up}(t)$, $M_{Down}(t)$ and $M_{Ini}(\xi)$, respectively, using (61), (62), (63) and (28). Finally, the unique solution is the smallest value:

$$M(\xi, t) = \min(M_{Up}(\xi, t), M_{Down}(\xi, t), M_{Ini}(\xi, t)). \quad (64)$$

Notice that in the following we will consider only solutions for large enough time

$$t \geq \max \left(\int_{\xi_{min}}^{\xi_{max}} \frac{1}{v_f(\hat{\xi})} d\hat{\xi}, \int_{\xi_{min}}^{\xi_{max}} \frac{1}{w(\hat{\xi})} d\hat{\xi} \right). \quad (65)$$

A. Upstream Boundary Condition

The solution $M_{Up}(\xi, t)$ is related to the number of vehicles originating from the upstream boundary ξ_{min} at initial time.

By definition of the value condition function (26) we get $c(\hat{\xi}(0), t - T) = M_{Up}(t - T)$ in (28). The upstream boundary condition is defined for ξ_{min} , which implies for $M_{Up}(\xi, t)$:

$$\hat{\xi}(0) = \xi_{min}, \quad \hat{\xi}(t) = \xi_{min} + \int_0^t v(\tau) d\tau. \quad (66)$$

Using (60) and (28), we formulate the following problem:

$$M_{Up}(\xi, t) = \inf_{(T, v) \in S_{Up}} \left[M_{Up}(t - T) + \int_0^T \phi_{max}(\hat{\xi}(\tau)) d\tau - \int_0^T \rho_c(\hat{\xi}(\tau)) v(\tau) d\tau \right],$$

where the infimum is taken over domain S_{Up} that is defined exactly as in (29) but with $(\hat{\xi}(0), t - T) \in \text{Dom}(c_{Up})$, where $c_{Up} = M_{Up}(t)$ as in (26).

With (61), the problem can be rewritten as

$$M_{Up}(\xi, t) = \inf_{(T, v) \in S_{Up}} \left[\int_0^{t-T} \phi_{in}(\tau) d\tau + \int_{\xi_{min}}^{\xi_{max}} \rho_0(\hat{\xi}) d\hat{\xi} + \int_0^T \phi_{max}(\hat{\xi}(\tau)) d\tau - \int_0^T \rho_c(\hat{\xi}(\tau)) v(\tau) d\tau \right]. \quad (67)$$

Now let us consider in more details the last term $\int_0^T \rho_c(\hat{\xi}(\tau)) v(\tau) d\tau$. By definition $d\hat{\xi} = v(\tau) d\tau$, which allows us to perform the following change of variables:

$$\int_0^T \rho_c(\hat{\xi}(\tau)) v(\tau) d\tau = \int_{\xi_{min}}^{\xi} \rho_c(\hat{\xi}) d\hat{\xi} =: R_c(\xi), \quad (68)$$

where $R_c(\xi)$ is a new variable that will be used to denote the cumulative critical density. Further, we can decompose the integrals in (67) as

$$\int_0^{t-T} \phi_{in}(\tau) d\tau + \int_0^T \phi_{max}(\hat{\xi}(\tau)) d\tau = \int_0^t \phi_{in}(\tau) d\tau + \int_0^T (\phi_{max}(\hat{\xi}(\tau)) - \phi_{in}(t - T + \tau)) d\tau. \quad (69)$$

Thus, using (68) and (69) we can rewrite (67) as

$$M_{Up}(\xi, t) = \inf_{(T, v) \in S_{Up}} \left[\int_0^T (\phi_{max}(\hat{\xi}(\tau)) - \phi_{in}(t - T + \tau)) d\tau + \int_0^t \phi_{in}(\tau) d\tau + \int_{\xi_{min}}^{\xi_{max}} \rho_0(\hat{\xi}) d\hat{\xi} - R_c(\xi) \right]. \quad (70)$$

By Assumption 1 we have $\forall(\xi, t) : \phi_{in}(t) \leq \phi_{max}(\xi)$. Hence, the infimum in (70) is achieved when T is minimized, which implies that velocity is maximal at each space point, i.e., (66) becomes

$$\hat{\xi}(t) = \xi_{min} + \int_0^t v_f(\tau) d\tau. \quad (71)$$

Thus, in the infimum T is the solution to (71) for $t = T$:

$$\frac{\partial \xi}{\partial T} = v_f(T) \Rightarrow \frac{\partial T}{\partial \xi} = \frac{1}{v_f(\xi)} \Rightarrow T_{v_f}(\xi) = \int_{\xi_{min}}^{\xi} \frac{1}{v_f(\hat{\xi})} d\hat{\xi}. \quad (72)$$

With (72) the viability solution related to the upstream boundary yields

$$M_{Up}(\xi, t) = \int_0^{T_{v_f}(\xi)} \phi_{max}(\hat{\xi}(\tau)) d\tau + \int_0^{t-T_{v_f}(\xi)} \phi_{in}(\tau) d\tau + \int_{\xi_{min}}^{\xi_{max}} \rho_0(\hat{\xi}) d\hat{\xi} - R_c(\xi). \quad (73)$$

We rewrite the first term on the right hand side of (73) as

$$\int_0^{T_{v_f}(\xi)} \phi_{max}(\hat{\xi}(\tau)) d\tau = \int_0^{T_{v_f}(\xi)} \rho_c(\hat{\xi}(\tau)) v_f(\hat{\xi}(\tau)) d\tau.$$

Using (71) we can perform the change of variables in the latter integral as

$$\int_0^{T_{v_f}(\xi)} \rho_c(\hat{\xi}(\tau)) v_f(\hat{\xi}(\tau)) d\tau = \int_{\xi_{min}}^{\xi} \rho_c(\hat{\xi}) d\hat{\xi} = R_c(\xi).$$

With this result two $R_c(\xi)$ terms with opposite signs cancel each other and we rewrite (73) as

$$M_{Up}(\xi, t) = \int_0^{t-T(\xi)} \phi_{in}(\tau) d\tau + \int_{\xi_{min}}^{\xi_{max}} \rho_0(\hat{\xi}) d\hat{\xi}. \quad (74)$$

B. Downstream Boundary Condition

As the second step we need to obtain $M_{Down}(\xi, t)$ that is related to the downstream boundary ξ_{max} . Notice that viable evolutions related to this boundary satisfy:

$$\hat{\xi}(0) = \xi_{max}, \quad \hat{\xi}(t) = \xi_{max} + \int_0^t v(\tau) d\tau. \quad (75)$$

As in the previous case, we use $M_{Down}(t)$ from (62) and the result from (69), and write the following infimum problem

$$M_{Down}(\xi, t) = \inf_{(T, v) \in S_{Down}} \left[\int_0^T (\phi_{max}(\hat{\xi}(\tau)) - \phi_{out}(t - T + \tau)) d\tau - \int_0^T \rho_c(\hat{\xi}(\tau)) v(\tau) d\tau + \int_0^t \phi_{out}(\tau) d\tau \right], \quad (76)$$

and the infimum is taken over domain S_{Down} defined as in (29) with $(\hat{\xi}(0), t - T) \in \text{Dom}(\mathbf{c}_{\text{Down}})$, where $\mathbf{c}_{\text{Down}} = M_{\text{Down}}(t)$ as in (26).

Again using Assumption 1, we obtain that in the infimum T should be minimized, which corresponds to:

$$T_w(\xi) = \int_{\xi}^{\xi_{max}} \frac{1}{w(\hat{\xi})} d\hat{\xi} \quad \text{and} \quad v = -w. \quad (77)$$

We use (77) and $\phi_{max} = \rho_c v_f$ to solve the infimum problem (76), which yields:

$$M_{\text{Down}}(\xi, t) = \int_0^{t-T_w(\xi)} \phi_{out}(\tau) d\tau + \int_0^{T_w(\xi)} \rho_c(\hat{\xi}(\tau)) v_f(\hat{\xi}(\tau)) d\tau + \int_0^{T_w(\xi)} \rho_c(\hat{\xi}(\tau)) w(\hat{\xi}(\tau)) d\tau. \quad (78)$$

From definition of the critical density for triangular FD we get

$$\rho_c = \frac{\rho_{max} w}{v_f + w} \Rightarrow \rho_{max} w = \rho_c (v_f + w),$$

which is then inserted into (78):

$$M_{\text{Down}}(\xi, t) = \int_0^{t-T_w(\xi)} \phi_{out}(\tau) d\tau + \int_0^{T_w(\xi)} \rho_{max}(\hat{\xi}(\tau)) w(\hat{\xi}(\tau)) d\tau.$$

Finally, we perform the change of variables

$$\int_0^{T_w(\xi)} \rho_{max}(\hat{\xi}(\tau)) w(\hat{\xi}(\tau)) d\tau = \int_{\xi}^{\xi_{max}} \rho_{max}(\hat{\xi}) d\hat{\xi}.$$

and thus obtain

$$M_{\text{Down}}(\xi, t) = \int_0^{t-T_w(\xi)} \phi_{out}(\tau) d\tau + \int_{\xi}^{\xi_{max}} \rho_{max}(\hat{\xi}) d\hat{\xi}. \quad (79)$$

C. Initial Condition

At the third step we need to calculate $M_{\text{Ini}}(\xi, t)$ that is related to the vehicle with known label at initial time that follows the path of viable evolution (see (63)).

We can already establish that $T = t$, since the viability evolution starts its path at initial time. Thus, using (28) with initial condition given by (63) we can state the infimum problem as

$$M_{\text{Ini}}(\xi, t) = \inf_{v \in S_{\text{Ini}}} \left[\int_{\hat{\xi}_0}^{\xi_{max}} \rho_0(\hat{\xi}) d\hat{\xi} + \int_0^t \phi_{max}(\hat{\xi}(\tau)) d\hat{\xi} - \int_0^t \rho_c(\hat{\xi}(\tau)) v(\tau) d\tau \right], \quad (80)$$

where the domain S_{Ini} is defined as in (29) for $T = t$:

$$S_{\text{Ini}} = \left\{ v \mid v(\cdot) \in L^1(0, t), \dot{\hat{\xi}}(\tau) = v(\tau), \hat{\xi}(t) = \xi, v(\tau) \in \left[-w(\hat{\xi}(\tau)), v_f(\hat{\xi}(\tau)) \right], \hat{\xi}(0) \in [\xi_{min}, \xi_{max}] \right\}. \quad (81)$$

In the first term of the right hand side of (80) the integral runs from $\hat{\xi}_0$ used to define the coordinate from which the viable evolution starts its path at initial time:

$$\hat{\xi}(0) = \hat{\xi}_0, \quad \hat{\xi}(t) = \hat{\xi}_0 + \int_0^t v(\tau) d\tau. \quad (82)$$

Again we use the change of variables such that $v(\tau) d\tau = d\hat{\xi}$ and rewrite (80) as

$$M_{\text{Ini}}(\xi, t) = \inf_{v \in S_{\text{Ini}}} \left[\int_{\hat{\xi}_0}^{\xi_{max}} \rho_0(\hat{\xi}) d\hat{\xi} - \int_{\hat{\xi}_0}^{\xi} \rho_c(\hat{\xi}) d\hat{\xi} + \int_0^t \phi_{max}(\hat{\xi}(\tau)) d\hat{\xi} \right]. \quad (83)$$

Let us now estimate the lower bound of (83) term by term:

$$M_{\text{Ini}}(\xi, t) \geq 0 - \int_{\xi_{min}}^{\xi_{max}} \rho_c(\hat{\xi}) d\hat{\xi} + \int_0^t \min \phi_{max} d\tau, \quad (84)$$

where $\min \phi_{max} = \min_{\xi \in [\xi_{min}, \xi_{max}]} \phi_{max}(\xi)$.

As already mentioned above, the unique solution (64) is the minimum among three functions. In the following section, we will show that starting from some time t_{min} , the initial conditions will have left the system and thus can be excluded from the minimum operator.

D. Time for Neglecting $M_{\text{Ini}}(\xi, t)$

Here we aim to estimate t_{min} such that $\forall (\xi, t) \in [\xi_{min}, \xi_{max}] \times [t_{min}, +\infty)$: $M_{\text{Ini}}(\xi, t) \geq M_{\text{Up}}(\xi, t)$ or $M_{\text{Ini}}(\xi, t) \geq M_{\text{Down}}(\xi, t)$. First, we will estimate the time after which $M_{\text{Ini}}(\xi, t) \geq M_{\text{Up}}(\xi, t)$, then we do the same for $M_{\text{Ini}}(\xi, t) \geq M_{\text{Down}}(\xi, t)$. Finally, t_{min} will be the smallest value of these two results.

Thus, we combine the result for $M_{\text{Up}}(\xi, t)$ (74) with the lower bound for $M_{\text{Ini}}(\xi, t)$ (84), and write

$$M_{\text{Ini}}(\xi, t) - M_{\text{Up}}(\xi, t) \geq - \int_{\xi_{min}}^{\xi_{max}} \rho_c(\hat{\xi}) d\hat{\xi} - \int_{\xi_{min}}^{\xi} \rho_0(\hat{\xi}) d\hat{\xi} + \int_0^{t-T_{v_f}(\xi)} (\min \phi_{max} - \phi_{in}(\tau)) d\tau + \int_0^{T_{v_f}(\xi)} \min \phi_{max} d\tau. \quad (85)$$

Now let us estimate lower bounds for the terms from (85) as

$$\int_0^{T_{v_f}(\xi)} \min \phi_{max} d\tau \geq 0, \quad - \int_{\xi_{min}}^{\xi_{max}} \rho_c(\hat{\xi}) d\hat{\xi} \geq \int_{\xi_{min}}^{\xi_{max}} \rho_{max}(\hat{\xi}) d\hat{\xi}.$$

which yields

$$M_{\text{Ini}}(\xi, t) - M_{\text{Up}}(\xi, t) \geq - \int_{\xi_{\min}}^{\xi_{\max}} \left(\rho_{\max}(\hat{\xi}) + \rho_c(\hat{\xi}) \right) d\hat{\xi} \\ + \int_0^{t-T_{v_f}(\xi)} (\min \phi_{\max} - \phi_{in}(\tau)) d\tau. \quad (86)$$

Using Assumption 2 we are able to estimate the following lower bound for the second term on the right hand side (86):

$$\int_0^{t-T_{v_f}(\xi)} (\min \phi_{\max} - \phi_{in}(\tau)) d\tau \geq \left[\frac{t-T_{v_f}(\xi)}{T_c} \right] \epsilon,$$

with $\epsilon > 0$ and T_c is from (32), which can be used to rewrite (86) as

$$M_{\text{Ini}}(\xi, t) - M_{\text{Up}}(\xi, t) \geq \left[\frac{t-T_{v_f}(\xi_{\max})}{T} \right] \epsilon \\ - \int_{\xi_{\min}}^{\xi_{\max}} \left(\rho_{\max}(\hat{\xi}) + \rho_c(\hat{\xi}) \right) d\hat{\xi}. \quad (87)$$

Now we can determine the minimal time for which the right hand side of (87) is non-negative:

$$t \geq \int_{\xi_{\min}}^{\xi_{\max}} \frac{1}{v_f(\hat{\xi})} d\hat{\xi} + \left[\frac{1}{\epsilon} \int_{\xi_{\min}}^{\xi_{\max}} \left(\rho_{\max}(\hat{\xi}) + \rho_c(\hat{\xi}) \right) d\hat{\xi} \right] T_c. \quad (88)$$

Afterwards, the same steps are performed to obtain the minimal time for which $M_{\text{Ini}}(\xi, t) - M_{\text{Down}}(\xi, t) \geq 0$ holds:

$$t \geq \int_{\xi_{\min}}^{\xi_{\max}} \frac{1}{w(\hat{\xi})} d\hat{\xi} + \left[\frac{1}{\epsilon} \int_{\xi_{\min}}^{\xi_{\max}} \left(\rho_{\max}(\hat{\xi}) + \rho_c(\hat{\xi}) \right) d\hat{\xi} \right] T_c. \quad (89)$$

Finally, t_{\min} is the minimum between (88) and (89):

$$t_{\min} = T_c \left(1 + \left[\frac{1}{\epsilon} \int_{\xi_{\min}}^{\xi_{\max}} \left(\rho_{\max}(\hat{\xi}) + \rho_c(\hat{\xi}) \right) d\hat{\xi} \right] \right). \quad (90)$$

E. Unique Solution $M(x, t)$

The final solution $M(\xi, t)$ can be obtained as a minimum between (74) and (79) $\forall t \in [t_{\min}, +\infty)$, thus, the effect of initial conditions is negligible:

$$M(\xi, t) = \min \left\{ \int_0^{t-T_{v_f}(\xi)} \phi_{in}(\tau) d\tau + \int_{\xi_{\min}}^{\xi_{\max}} \rho_0(\hat{\xi}) d\hat{\xi}, \right. \\ \left. \int_0^{t-T_w(\xi)} \phi_{out}(\tau) d\tau + \int_{\xi}^{\xi_{\max}} \rho_{\max}(\hat{\xi}) d\hat{\xi} \right\}.$$

APPENDIX II

DIFFERENCES IN THE PROOFS

Due to the space dependence in the fundamental diagram, the proof in [42] should be modified by taking the following differences into account (here we again write all the dependencies on parameter η in the notations but still omit bars):

- 1) Space intervals for a 1D road of length L vary as a function of line number η , i.e., $[0, L] \rightarrow [\xi_{\min}(\eta), \xi_{\max}(\eta)]$. This implies that $\frac{L}{v_f} \rightarrow T_{v_f}(\xi_{\max}, \eta)$ and $\frac{L}{w} \rightarrow T_w(\xi_{\min}, \eta)$ where $T_{v_f}(\xi_{\max}, \eta)$ and $T_w(\xi_{\min}, \eta)$ should be taken from (34) for $\xi = \xi_{\max}$ and $\xi = \xi_{\min}$, respectively.
- 2) Every occurrence of $L\rho_{\max}$ should be substituted by $\int_{\xi_{\min}(\eta)}^{\xi_{\max}(\eta)} \rho_{\max}(\hat{\xi}, \eta) d\hat{\xi}$.
- 3) Equation (29) of [42] should be rewritten as:

$$g_{in}(\eta, t) = 0 \Rightarrow \\ R(\eta, t') \geq \int_{\xi_{\min}(\eta)}^{\xi_{\max}(\eta)} \rho_c(\hat{\xi}, \eta) d\hat{\xi} \quad \forall t' \in [t - T_w(\xi_{\min}, \eta), t], \\ g_{out}(\eta, t) = 0 \Rightarrow \\ R(\eta, t') \leq \int_{\xi_{\min}(\eta)}^{\xi_{\max}(\eta)} \rho_c(\hat{\xi}, \eta) d\hat{\xi} \quad \forall t' \in [t - T_{v_f}(\xi_{\max}, \eta), t]. \quad (91)$$

We obtain (91) by using the following upper bound:

$$\int_{t-T_w(\xi_{\min}, \eta)}^{t'} \phi_{out}(\eta, \tau) d\tau + \int_{t'}^t \phi_{in}(\eta, \tau) d\tau \leq \\ T_w(\xi_{\min}, \eta) \min \phi_{\max} \leq \int_{\xi_{\min}(\eta)}^{\xi_{\max}(\eta)} \frac{\phi_{\max}(\hat{\xi}, \eta)}{w(\hat{\xi})} d\hat{\xi} \\ = \int_{\xi_{\min}(\eta)}^{\xi_{\max}(\eta)} \left(\rho_{\max}(\hat{\xi}, \eta) - \rho_c(\hat{\xi}, \eta) \right) d\hat{\xi}.$$

REFERENCES

- [1] G. Lamé, "Leçons sur les coordonnées curvilignes et leurs diverses applications", Paris, France 1859.
- [2] M. Lighthill and G. Whitham, "On kinematic waves, II: A theory of traffic flow on long crowded roads", *Proc. Royal Soc. London*, vol. 229, no. 1178, pp. 317-345, 1956.
- [3] P. Richards, "Shock waves on the highway", *Operations Res.*, vol. 47, no. 1, pp. 42-51, 1956.
- [4] S. K. Godunov, "A difference method for numerical calculation of discontinuous solutions of the equations of hydrodynamics", *Matematicheskii Sbornik*, vol. 47, no. 3, pp. 271-306, 1959.
- [5] K. Moskowitz, "Discussion of freeway level of service as influenced by volume and capacity characteristics by dr drew and cj keese" in *Proc. Highway Research Record*, 1965, vol. 99, pp. 43-44.
- [6] R. J. Smeed, "The road capacity of city centers", *Traffic Engineering and Control*, vol. 8, pp. 455-458, 1966.
- [7] R. Courant, K. Friedrichs and H. Lewy, "On the Partial Difference Equations of Mathematical Physics", *IBM Journal of Research and Development*, vol. 11, no. 2, 1967.
- [8] J.M. Thomson, "Speeds and flows of traffic in Central London: 2. Speed-flow relations" *Traf. Eng. and Control*, vol. 8, pp. 721-725, 1967.
- [9] R. Herman and I. Prigogine, "A two-fluid approach to town traffic", *Science*, vol. 204, pp. 148-151, 1979.

- [10] M. Papageorgiou, H. Hadj-Salem and J. Blosseville, "ALINEA: a local feedback control law for on-ramp metering", *Transp. Res. Rec.*, vol. 1320, pp. 58-64, 1991.
- [11] G. Newell, "A simplified theory of kinematic waves in highway traffic, part i,ii and iii", *Trans. Res. B: Meth.*, vol. 27, no. 4, pp. 281-287, 1993.
- [12] C. F. Daganzo, "The cell transmission model: A dynamic representation of highway traffic consistent with the hydrodynamic theory", *Transportation Research Part B: Methodological*, vol. 28, no. 4, pp. 269-287, 1994.
- [13] M. Papageorgiou, C. Diakaki, V. Dinopoulou, A. Kotsialos and Y. Wang, "Review of Road Traffic Control Strategies", *Proc. IEEE*, vol. 91, no. 12, pp. 2043-2067, Dec. 2003.
- [14] A. K. Ziliaskopoulos, S. T. Waller, Y. Li, M. Byram, "Large-scale dynamic traffic assignment: implementation issues and computational analysis", *J. Transp. Eng.*, vol. 130, no. 5, pp. 585-593, 2004.
- [15] C. F. Daganzo, "A variational formulation of kinematic waves: basic theory and complex boundary conditions", *Transportation Research Part B: Methodological*, vol. 39, no. 2, pp. 187-196, 2005.
- [16] C. F. Daganzo, "A variational formulation of kinematic waves: solution methods", *Transportation Research Part B: Methodological*, vol. 39, no. 10, pp. 934-950, 2005.
- [17] M. Gugat, M. Herty, A. Klar and G. Leugering, "Optimal control for traffic flow networks", *J. Opt. Th. Appl.*, vol. 126 (3), pp. 589-616, 2005.
- [18] J. P. Lebacque, "First-order macroscopic traffic flow models: Intersection modeling, network modeling", in *16th Int. Symp. Transp. Traffic Theory*, 2005, pp. 365-386.
- [19] C. F. Daganzo, "On the variational theory of traffic flow: Well-posedness, duality and applications", *Netw. Heter. Med.*, vol. 1, pp. 601-619, 2006.
- [20] M. Garavello and B. Piccoli, *Traffic flow on networks*, Springfield, MO: Amer. Inst. Math. Sci., 2006.
- [21] I. Strub and A. Bayen, "Weak formulation of boundary conditions for scalar conservation laws: An application to highway traffic modelling", *Int. J. Robust Nonlinear Control*, vol. 16, no. 4, pp. 733-748, 2006.
- [22] J-P. Aubin, A. Bayen and P. Saint-Pierre, "Dirichlet problems for some Hamilton-Jacobi equations with inequality constraints", *SIAM J. Control Optim.*, vol. 47, no. 5, pp. 2348-2380, 2008.
- [23] C. F. Daganzo and N. Geroliminis, "An analytical approximation for the macroscopic fundamental diagram of urban traffic", *Transportation Research Part B: Methodological*, vol. 42, pp. 771-781, 2008.
- [24] N. Geroliminis and C.F. Daganzo, "Existence of urban-scale macroscopic fundamental diagrams: Some experimental findings", *Transportation Research Part B: Methodological*, vol. 42, pp. 756-770, 2008.
- [25] M. Z. F. Li, "A generic characterization of equilibrium speed-flow curves", *Transportation Science*, vol. 42, no. 2, pp. 220-235, 2008.
- [26] M. Papageorgiou, E. Kosmatopoulos and I. Papamichail, "Effects of variable speed limits on motorway traffic flow", *Trans. Res. Record*, vol. 2047, pp. 37-48, 2008.
- [27] M. Garavello and B. Piccoli, "Conservation laws on complex networks", *Ann. Inst. Henri Poincaré, Anal. Non Lin.*, vol. 26, pp. 1925-1951, 2009.
- [28] R. Carlson, I. Papamichail, M. Papageorgiou and A. Messmer, "Optimal Motorway Traffic Flow Control Involving Variable Speed Limits and Ramp Metering", *Transp. Sci.*, vol. 44, no. 2, pp. 238-253, 2010.
- [29] J-P. Aubin, A. Bayen and P. Saint-Pierre, *Viability Theory: New Directions*, Springer, 2011.
- [30] A. Désilles, "Viability approach to Hamilton-Jacobi-Moskowitz problem involving variable regulation parameters", *American Institute of Math. Sci.*, vol. 8, no. 3, pp. 707-726, 2012.
- [31] K. Aboudolas and N. Geroliminis, "Perimeter and boundary flow control in multi-reservoir heterogeneous networks", *Transportation Research Part B: Methodological*, vol. 55, pp. 265-281, 2013.
- [32] M. Hajjahmadi, V. L. Knoop, B. De Schutter and H. Hellendoorn, "Optimal dynamic route guidance: A model predictive approach using the macroscopic fundamental diagram", in *16th Int. IEEE ITS Conf.*, 2013, pp. 1022-1028.
- [33] S. Goettlich and U. Ziegler, "Traffic light control: a case study", *Intelligent Transportation Systems-(ITSC), Discrete Cont. Dyn. Syst., Ser. S*, vol. 7, pp. 483-501, 2014.
- [34] F. van Wageningen-Kessels, H. van Lint, K. Vukic and S. Hoogendoorn, "Genealogy of traffic flow models", *EURO Journal on Transportation and Logistics*, vol. 4, pp. 445-473, 2015.
- [35] L. Leclercq, C. Parzani, V. L. Knoop, J. Amourette and S. P. Hoogendoorn, "Macroscopic traffic dynamics with heterogeneous route patterns", *Transportation Research Procedia*, vol. 7, pp. 631-650, 2015.
- [36] M. L. Delle Monache, B. Piccoli and F. Rossi, "Traffic Regulation via Controlled Speed Limit", *SIAM J. Control Optim.*, vol. 55, no. 5, pp. 2936-2958, 2017.
- [37] S. Mollier, M. L. Delle Monache and C. Canudas-de-Wit, "Two-dimensional macroscopic model for large scale traffic networks", *Transportation Research Part B: Methodological*, vol. 122, pp. 309-326, 2019.
- [38] I. Karafyllis and M. Papageorgiou, "Feedback control of scalar conservation laws with application to density control in freeways by means of variable speed limits", *Automatica*, vol. 105, pp. 228-236, 2019.
- [39] R. Aghamohammadi and J. A. Laval, "Dynamic traffic assignment using the macroscopic fundamental diagram: A Review of vehicular and pedestrian flow models", *Transportation Research Part B: Methodological*, vol. 137, pp. 99-118, 2020.
- [40] L. Tumash, C. Canudas-de-Wit and M. L. Delle Monache, "Equilibrium Manifolds in 2D Fluid Traffic Models", *21th IFAC World Congress*, Berlin, Germany, 2020, hal-02513273v2f.
- [41] L. Tumash, C. Canudas-de-Wit and M.L. Delle Monache, "Topology-based control design for congested areas in urban networks", *ITSC 2020 - 23rd IEEE Int. Conf. Intel. Transp. Sys.*, Rhodes, Greece, Sep. 2020, <https://hal.archives-ouvertes.fr/hal-02860455v2/document>.
- [42] L. Tumash, C. Canudas-de-Wit and M.L. Delle Monache, "Boundary Control Design for Traffic with Nonlinear Dynamics", accepted to IEEE TAC, 2020, available: <https://hal.archives-ouvertes.fr/hal-02955853/document>.



Liudmila Tumash received both the B.Sc. and the M.Sc. degree in Institute of Theoretical Physics from the Technical University of Berlin, Berlin, Germany, specialising on control of chaotic networks. She was the recipient of Physik-Studienpreis for the excellent Master's degree.

She is currently a doctoral researcher at CNRS, Gipsa-Lab, Grenoble, France. Her research mainly focuses on control of traffic systems in large-scale networks.



Carlos Canudas-de-Wit (F'16) was born in Villahermosa, Mexico, in 1958. He received the B.S. degree in electronics and communications from the Monterrey Institute of Technology and Higher Education, Monterrey, Mexico, in 1980, and the M.S. and Ph.D. degrees in automatic control from the Department of Automatic Control, Grenoble Institute of Technology, Grenoble, France, in 1984 and 1987, respectively. He is currently a Directeur de recherche (Senior Researcher) with CNRS, Grenoble, where he is the Leader of the NeCS Team, a joint team of GIPSA-Lab (CNRS) and INRIA, on networked controlled systems.

Dr. Canudas-de-Wit is an IFAC Fellow. He was an Associate Editor of the IEEE Transactions on Automatic Control, the Automatica, the IEEE Transactions on Control Systems Technology. He is an Associate Editor of the Asian Journal of Control, and the IEEE Transactions on Control of Network Systems. He served as the President of the European Control Association from 2013 to 2015, and a member of the IEEE Board of Governors of the Control System Society from 2011 to 2014. He holds the ERC Advanced Grant Scale-FreeBack from 2016 to 2021.



Maria Laura Delle Monache is a research scientist in the Networked Controlled Systems team at Inria and in GIPSA-Lab (Department of Control) in Grenoble. She received the B.S. degree in industrial engineering from the University of L'Aquila, L'Aquila, Italy, the M.S. degree in mathematical engineering from the University of L'Aquila, and the Ph.D. degree in applied mathematics from the University of Nice-Sophia Antipolis, Nice, France in 2009, 2011, and 2014,

respectively. Prior to Inria, she was a Postdoctoral researcher at Rutgers University Camden. Her research interest is mainly related to mathematical and engineering aspects of traffic flow. In particular, she is interested in mathematical modeling and control of traffic flow applications.